AD A108880

AFGL-TR-81-0289

(12)

LEVEL II

THE ESTIMATION OF FREE-AIR ANOMALIES

Hans Sünkel

Department of Geodetic Science and Surveying
The Ohio State University
Columbus, Ohio 43210

Scientific Report No. 9

September 1981

Approved for public release; distribution unlimited

AIR FORCE GEOPHYSICS LABORATORY
AIR FORCE SYSTEMS COMMAND
UNITED STATES AIR FORCE
HANSCOM AFB, MASSACHUSETTS 01731

Unclassified

SECURITY CLASSIFICATION OF THIS PAGE (When Data Entered)

REPORT DOCUMENTATION PAGE		READ INSTRUCTIONS BEFORE COMPLETING FORM
1. REPORT NUMBER AFGL-TR-81-0289	2. GOVT ACCESSION NO. AD-A108 880	3. RECIPIENT'S CATALOG NUMBER
4. TITLE (and Subtitle) THE ESTIMATION OF FREE-AIR ANOMALIES		5. TYPE OF REPORT & PERIOD COVERED Scientific Report No. 9
		6. PERFORMING ORG. REPORT NUMBER Report No. 315
7. AUTHOR(s) Hans Sünkel		8. CONTRACT OR GRANT NUMBER(s) F19628-79-C-0075
9. PERFORMING ORGANIZATION NAME AND ADDRESS Department of Geodetic Science and Surveying The Ohio State University Columbus, Ohio 43210		10. PROGRAM ELEMENT, PROJECT, TASK AREA & WORK UNIT NUMBERS 62101F 760003AL
11. CONTROLLING OFFICE NAME AND ADDRESS Air Force Geophysics Laboratory Hanscom AFB, Massachusetts 01731 Contract Monitor: Bela Szabo/LW		12. REPORT DATE September 1981
		13. NUMBER OF PAGES 71 pages
14. MONITORING AGENCY NAME & ADDRESS (if different from Controlling Office)		15. SECURITY CLASS. (of this report) Unclassified
		15a. DECLASSIFICATION/DOWNGRADING SCHEDULE

16. DISTRIBUTION STATEMENT (of this Report)

Approved for public release; distribution unlimited

17. DISTRIBUTION ST[ATEM]ENT (of [the] abstract entered in Block 20, if different from Report)

18. SUPPLEMENTARY [NO]TES

19. KEY WORDS (Continue on reverse side if necessary and identify by block number)

Free-air anomalies	Least-squares collocation
Bouguer anomalies	Isostasy
Linear correlation	Terrain effect

20. ABSTRACT (Continue on reverse side if necessary and identify by block number)

A prediction model of point and/or mean free-air anomalies, based on point values, is proposed. It relies on the concept of least-squares collocation with parameters. The model parameters are the two regression parameters of a linear model, which assumes a linear correlation between free-air anomaly and elevation. Particular emphasis is put on the role of the topography in mountainous areas.

DD FORM 1 JAN 73 1473

Unclassified

SECURITY CLASSIFICATION OF THIS PAGE (When Data Entered)

Foreword

This report was prepared by Dr. Hans Sünkel, Technical University at Graz, Austria, under Air Force Contract No. F19628-79-C-0075, The Ohio State University Research Foundation, Project No. 711715, Project Supervisor, Urho A. Uotila, Professor, Department of Geodetic Science and Surveying. The contract covering this research is administered by the Air Force Geophysics Laboratory (AFGL), Hanscom Air Force Base, Massachusetts, with Mr. Bela Szabo/LW, Contract Monitor.

CONTENTS

1. INTRODUCTION

Why do we need another paper on the estimation of point and mean free-air gravity anomalies based on point gravity measurements? Isn't this subject settled once and for all? We do have the omnipotent tool called least-squares collocation, even with parameters.

These and others are typical questions and arguments of the seventies, when the geodetic community became aware of and excited about the existence of collocation. Some enthusiastic proponents (not its designers, mind you) advertised it as the unique robot, which is capable of making even the impossible come true; but unfortunately it doesn't. Meanwhile the enthusiasm has been replaced by an "unbiased" recognition of this sound and powerful tool; practical experience has shown what could have been anticipated: a smooth and reliable output requires a smooth, detailed and accurate input - the system's response is data - specific.

One of the many applications of least-squares collocation is the prediction of point and mean gravity anomalies based on point gravity anomalies - hardly any problem, as long as the terrain is flat within the area of consideration. Free-air anomalies can be processed directly, no data reduction seems to be necessary. If we approach the foothills or even mountainous areas, the picture changes dramatically; suddenly data reduction becomes indispensable, collocation results based on unreduced quantities become practically useless.

This report aims at an optimal estimation of point and mean anomalies taking into account the concept of a linear correlation between terrain-corrected free-air anomalies and topographic height. Different

estimation procedures are compared; particular emphasis is put on the best possible estimation of the Bouguer-factor and the subsequent estimation of Bouguer as well as free-air point and mean anomalies. Least-squares collocation with parameters presents itself as a very attractive and powerful tool for the estimation of both regression parameters and point and/or mean anomalies. An explanation for the regional variation of the regression parameters, based on a simplified concept of isostatic compensation is presented in chapter 4.

Particularly in mountainous areas the free-air anomalies used to be reduced for the effect of the terrain, which can easily attain values of 10-20 mgals and even more. If an empirical covariance function is estimated from unreduced free-air anomalies, the terrain effect causes the variance to be too high and the correlation length to be too short. Since the variance functions as a scale factor for the prediction error, we see that the quality of anomaly prediction is worsened if unreduced free-air anomalies are used. In addition, the correlation length controls the quality of interpolation; a short correlation length causes a large prediction (interpolation) error; therefore, the prediction accuracy suffers also from this indirect effect (cf. Sünkel, 1981). The estimation of the terrain effect is a very laborious task. It is shown in chapters 5 and 6 to depend linearly on the terrain variance and to be inverse proportional with respect to wavelength and correlation length, respectively. The total variance depends on the power spectrum; if the high frequency part of the spectrum has much power, a high terrain sampling rate (= detailed terrain model) is required in order to estimate the variance with sufficient accuracy. The terrain correlation length plays a fundamental role in the estimation of the mean terrain effect; a short

correlation length requires a high sampling rate. As a matter of fact, these statistical quantities depend strongly on the terrain in consideration; consequently, a globally valid sampling rate cannot be given; individual circumstances control its choice.

2. MEAN FREE-AIR GRAVITY ANOMALIES

A free-air gravity anomaly is defined by

$$\Delta g_P = g_P - \gamma_Q , \tag{2.1}$$

with g_P denoting the actual gravity at the point P located on the surface of the earth, and γ_Q denoting the reference gravity at a corresponding point Q located on the telluroid (Heiskanen & Moritz, 1967, p. 293). By $\Delta\bar{g}$ we denote a mean value of the free-air gravity anomaly,

$$\Delta\bar{g}_P = \frac{1}{\Delta\sigma_P} \iint_{\Delta\sigma_P} \Delta g_{P'} \, d\sigma_{P'} ; \tag{2.2}$$

$d\sigma$ stands for the element of solid angle, $\Delta\sigma$ is the averaging area in consideration.

Point free-air anomalies are known to oscillate around a zero average with oscillation frequencies depending strongly on the topographical features; they comprise regional and local gravity field information; therefore, a point anomaly is in general not representative for a large area; because of its local character and its strong dependence on topography, it can only be poorly predicted if the topography is ignored (this is particularly true for mountainous areas).

Averaging free-air anomalies in order to obtain mean anomalies means essentially averaging the local features of free-air anomalies; mean anomalies are representative for the averaging area in consideration; they offer themselves for the evaluation of various integral formulas.

Applying the averaging process (2.2) we have to keep in mind that the free-air anomalies refer to ground level,

$$\Delta g_P = \Delta g \left(\phi_P, \lambda_P, h\,(\phi_P, \lambda_P)\right) ; \tag{2.3}$$

$\big(h(\phi,\lambda)$ denotes the topography.$\big)$ A straight mean like (2.2) is taken with respect to the horizontal position (ϕ,λ); to which height does $\Delta\bar{g}_p$ refer? Does it refer to a mean height?

In order to answer this question we introduce a mean height $\bar{h}$ by

$$\bar{h}_p = \frac{1}{\Delta\sigma_p} \iint_{\Delta\sigma_p} h_{p'} d\sigma_{p'} \quad . \tag{2.4}$$

Let us introduce a mean anomaly $\Delta\bar{g}^*$, which refers to the mean height h; $\Delta\bar{g}^*$ is a mean of point anomalies Δg^*, which refer to the level $h = \bar{h}$ and are obtained by an anlytical continuation of the ground level anomalies,

$$\Delta g^* = \Delta g - \frac{\partial \Delta g}{\partial h}(h - \bar{h}), \tag{2.5a}$$

$$\Delta\bar{g}^*_p = \frac{1}{\Delta\sigma_p} \iint_{\Delta\sigma_p} \Delta g^*_{p'}\, d\sigma_{p'} \quad . \tag{2.5b}$$

Denoting the average (2.2) by $M\{\cdot\}$, the mean anomaly referred to the mean height becomes

$$\Delta\bar{g}^* = \Delta\bar{g} + \bar{h}\, M\left\{\frac{\partial\Delta g}{\partial h}\right\} - M\left\{\frac{\partial\Delta g}{\partial h}\, h\right\} \ . \tag{2.6}$$

It is instructive to consider two special cases:

a) the trivial case of a flat topography within the area of averaging, $h = \bar{h}$; it is obvious that the last two terms of (2.6) cancel each other, and

$$\Delta\bar{g} = \Delta\bar{g}^*$$

follows. The straigt mean of free-air anomalies refers to the mean height.

b) the vertical gradient $\partial\Delta g/\partial h$ is constant within the area of averaging, $\partial\Delta g/\partial h = M\{\partial\Delta g/\partial h\}$. Again, the last two terms of (2.6) cancel each other, and

$$\Delta\bar{g} = \Delta\bar{g}^*$$

follows. The straight mean refers to the mean height.

The last case is of particular importance because it assumes a linear relation (= exact functional dependence) between Δg and h. In reality, local density anomalies, non-constant Bouguer-anomalies (in the averaging area), nearby topographic irregularities, and other phenomena account for the disturbance of an exact functional dependence; however, in general we observe a linear correlation (approximate linear relation) between Δg and h, which becomes even more ponounced if Δg is "cleaned" from topographical irregularities. We have hardly ever a sufficiently dense gravity material which would allow a determination of the vertical gradient of gravity; therefore, we simply have to assume that

$$M \left\{ \frac{\partial \Delta g}{\partial h} (h - \bar{h}) \right\}$$

is zero, in other words, the straight mean of point anomalies $\Delta \bar{g}$ is interpreted as $\Delta \bar{g}^*$ and consequently, the reference height becomes the mean height. In areas with flat topography the equality holds exactly.

3. PREDICTION OF ANOMALIES BY TREND REMOVAL

Adopting the concept of linear correlation between free-air anomaly and topographic height, the anomaly can be represented by

$$\Delta g_p = a + bh_p + s_p \ , \tag{3.1}$$

where a denotes a regional constant and s a residual anomaly; s comprises all the effects which make Δg locally violate the linear functional relations; the average of s is assumed to be zero,

$$M\{s\} = 0 \ . \tag{3.2}$$

Then the average of the mean value reduced anomalies Δg^r,

$$\begin{aligned} \Delta g_p^r &= \Delta g_p - M\{\Delta g\} \\ &= b\,(h_p - M\{h\}) + s_p \ , \end{aligned} \tag{3.3}$$

vanishes, $M\{\Delta g^r\} = 0$.

Introducing a reduced height h^r,

$$h_p^r = h_p - M\{h\} \ , \tag{3.4}$$

the reduced anomaly is represented as

$$\Delta g_p^r = bh_p^r + s_p \ . \tag{3.3$'$}$$

If s is to be independent of elevation, it follows that the covariances cov $(\Delta g^r, h^r)$ and cov (h^r, h^r) are proportional to each other for all arguments with b being the factor of proportionality (Heiskanen & Moritz, 1967, p. 283 ff.) ,

$$b = \frac{\mathrm{cov}\,(\Delta g^r, h^r)}{\mathrm{cov}\,(h^r, h^r)} \ . \tag{3.5}$$

Having selected a best-fitting b, the signal s can be predicted at any other point by well-established least-squares prediction methods. A

free air anomaly at a specific point Q at an elevation h_Q is obtained by

$$\Delta g_Q = M\{\Delta g\} + b\,(h_Q - M\{h\}) + s_Q \tag{3.6}$$

or shortly

$$\Delta g_Q = a + bh_Q + s_Q \tag{3.6a}$$

with a determined through

$$a = M\{\Delta g\} - bM\{h\}\ . \tag{3.6b}$$

At this point it should be stressed that the average $M\{\cdot\}$ is always derived from a finite sample of data (free-air anomalies, topographic heights); this fact will not cause any problems as long as the terrain is sufficiently flat; (the average over a perfectly flat terrain is obtained by a single data.) However, in mountainous areas the situation is quite different: gravity measurements are usually performed along main leveling lines which, in turn, almost exclusively coincide with main roads running through valleys rather than on the top of the mountains. Therefore, the estimate $M\{h\}$ will tend to be too low, and since the free-air anomalies are linearly correlated with height, the estimate $M\{\Delta g\}$ tends to be too low as well. The direct effect on the point anomaly prediction would be negligible provided the gravity gradient b is sufficiently well determined. However, the estimation of b is poor if the height range of the data is narrow. Therefore, sampling gravity and corresponding height in valleys only will make point predictions very inaccurate. A homogeneous sampling is therefore strongly recommended.

A mean anomaly $\Delta\bar{g}$ can be derived immediately from (3.6),

$$\Delta\bar{g} = M\{\Delta g\} + b\,(\bar{h} - M\{h\}), \tag{3.7}$$

provided the average of the signal s vanishes. Again we observe that the uncertainty of b enters directly in the uncertainty of the mean value. Practical results (Uotila, 1967 a,b; Sünkel und Malits, 1981) indicate that b can be estimated with an error ranging from $\pm 10^{-3}$ to $\pm 10^{-2}$ mgal/m; therefore, a difference $\Delta h = \bar{h} - M\{h\}$ of a couple of hundred meters (a case quite likely in mountainous areas) can contribute to the error budget of $\Delta\bar{g}$ by a couple of mgals.

As far as the estimation of a and b is concerned, either a classical least-squares fit (Uotila, 196, a,b) or a more demanding least-squares collocation solution can be envisioned. The least-squares estimation of the parameters a and b (trend model parameters) is performed by considering s as random noise. Denoting the parameter vector by X and the design matrix by A,

$$X^T = (a, b) \ , \ A^T = \begin{bmatrix} 1, 1, \ldots, 1 \\ h_1, h_2, \ldots, h_n \end{bmatrix}$$

the best estimate of X is obtained by

$$\hat{X} = (A^T A)^{-1} A^T \Delta g; \tag{3.8}$$

its elements can easily be shown to equal

$$\hat{b} = \frac{\sum_{i=1}^{n} h_i^r \, \Delta g_i}{\sum_{i=1}^{n} (h_i^r)^2} \ , \ \hat{a} = M\{\Delta g\} - bM\{h^r\} \ . \tag{3.8$'$}$$

The least-squares collocation solution differs from the simple least-squares solution insofar as it also takes into account the statistical behavior of the signal s (which is for sure not simply random noise), expressed in terms of its covariance function. The best estimate of the parameter vector X is now given by

$$\hat{X} = (A^T C^{-1} A)^{-1} A^T C^{-1} \Delta g \tag{3.9}$$

where C denotes the covariance matrix of the vector of signals. Therefore, the two solutions will differ, if the individual signals are correlated.(C has non-vanishing off-diagonal elements.) It need not to be mentioned that the collocation solution (3.9) is by far more expensive than the least-squares solution (3.8), because it requires a) an estimation of an empirical covariance function of the signal s, b) the fit of an appropriate model to the empirical covariance function, c) the calculation of $[n\ (n-1)]/2$ covariances, and d) the inversion of the covariance matrix. This is the price we have to pay for an optimal estimate obtainable from the available data set. The price will be definitely too high if the correlation between the signals is very weak (almost diagonal covariance matrix), it will be a good investment if the correlations are strong: practical studies have shown (Sünkel and Malits, 1981) that the variance of the signal can be quite considerable (easily reach 100 mgal and more); this variance enters unreduced into the error estimate of the point anomaly if the simple least-squares concept is applied. In the least-squares collocation method the predicted signal is obtained from the centered data by the well-known relation

$$\hat{s}_Q = C_Q^T\, C^{-1}\, (\Delta g - A\hat{x}); \tag{3.10}$$

the error covariance matrix E_{SS} of the predicted signal vector s is given by

$$E_{SS} = C_{SS} - C_S^T C^{-1} \left[I - A(A^T C^{-1} A)^{-1} A^T C^{-1} \right] C_S \quad , \tag{3.11}$$

the error covariance matrix of the predicted parameter vector by

$$E_{xx} = (A^T C^{-1} A)^{-1} \tag{3.12}$$

(Moritz, 1980, p. 128). Equation (3.11) can be split up into three terms,

$$E_{ss} = C_{ss} - C_s^T C^{-1} C_s + (A^T C^{-1} C_s)^T E_{xx} \, (A^T C^{-1} C_s) \ ;$$

the first term represents the a priori error (covariance matrix) of the estimated signal vector, the second term represents the accuracy gain due to data, and the third term the contribution of the parameter inaccuracies to the error of the estimated signal. As a general rule it can be said that a strong signal variance, a small correlation length compared to the mean mutual distance between data, and a vague linear correlation between Δg and h will be responsible for poor signal accuracies; a low variance, long correlation length, and a strong linear correlation will keep the prediction error low.

Any other free-air point gravity anomaly can be estimated through

$$\Delta\hat{g}_Q = A_Q \hat{X} + \hat{s}_Q \tag{3.13}$$

where A denotes the design vector corresponding to the prediction point Q,

$$A_Q^T = (1, \, h_Q) \ . \tag{3.14}$$

The mean square estimation error is obtained by

$$m^2_{\Delta g_Q} = A_Q E_{xx} A_Q^T + A_Q E_{xs} + E_{xs} A_Q^T + E_{ss} \tag{3.15a}$$

with the error cross covariance matrix

$$E_{xs} = -(A^T C^{-1} A)^{-1} A^T C^{-1} C_s \ . \tag{3.15b}$$

Equation (3.13) enables us to estimate the mean free-air anomaly through

$$\hat{\bar{\Delta g}} = \bar{A}_o \hat{X} + \hat{\bar{s}}_o \ , \tag{3.16}$$

where $\bar{A}_o$ denotes the mean of all vectors (3.14) which is obviously

$$\bar{A}_o = (1, \bar{h}) \ .$$

The estimated mean anomaly refers to the mean height; if the mean of the signal vanishes, we obtain

$$\hat{\bar{\Delta g}} = \hat{a} + \hat{b}\ \bar{h} \tag{3.17}$$

as best linear unbiased estimate of the mean gravity anomaly. (Note that it makes no difference if we take the mean of the surface anomalies or the mean of the anomalies at mean height; this is because the signal was supposed to be uncorrelated with height.) Formally (3.17) is valid for both, the adjustment solution and the least-squares collocation solution; however, the way the estimates $\hat{a}$ and $\hat{b}$ are obtained is different.

The collocation solution is based on the covariance function of the signal s; therefore, it would be quite interesting to know which kind of information is contained in s. According to its definition (3.1), s is a kind of mean value reduced Bouguer anomaly with the parameter a as the (constant) mean Bouguer anomaly in the area of consideration and b the Bouguer factor which can be related to the mean density ρ by $b = 2\pi G\rho$ (G is the gravitational constant). Since no terrain correction has been taken into account in our model, the signal s will comprise essentially 3 kinds of information:

a) the variation of the Bouguer anomaly within the area of consideration,

b) the terrain effect,

c) the effect of local and regional density anomalies.

Terrain corrected Bouguer anomalies Δg_B are known to be very smooth and correlated to a "mean" height $\tilde{h}$ such that in average

$$\Delta g_B = -100 \cdot \tilde{h} \, [\mathrm{km}] \text{ mgal} \tag{3.18}$$

(Heiskanen & Moritz, 1967, p. 328); the definition of "mean" is strongly linked to the concept of isostasy which will be discussed in the next chapter. If the terrain is rough, the behavior of the terrain correction will be similarly rough and high-frequent. Since no terrain correction has been applied, the signal s will have a long-wavelength Bouguer anomaly characteristic superimposed by a short-wavelength terrain effect characteristic; density anomalies will probably cover the whole spectrum as far as its effect on the signal is concerned however, its power is considered to be rather small compared to the Bouguer and terrain effect.

In moderately rough areas the terrain effect will be small and the signal is essentially a Bouguer anomaly. It is true that Bouguer anomalies are smooth (*cf.* (3.18)), but still they are hardly ever constant in an area of say $1^o \times 1^o$; its variation enters fully into the signal s. What is the impact of the relation (3.18) on a determination of the parameter b by least-squares adjustment? Very simple, the value of b will tend to decrease with increasing area of consideration. Why? As we saw earlier, s is essentially a Bouguer anomaly which behaves according to (3.18),

$$s \approx \Delta g_B + \text{const.} \approx -0.1 \cdot \tilde{h}\ [\text{m}] + \text{const.},$$

and consequently, the free-air anomaly is approximately given by

$$\Delta g_P \approx bh_P - 0.1\tilde{h}_P + \text{const.},$$

and with homogenous density $\rho = 2.67\ \text{g cm}^{-3}$,

$$\Delta g_P \approx 0.1(h - \tilde{h})_P + \text{const.} \quad (3.19)$$

Consider a region of $1^\circ \times 1^\circ$, subdivide it into 9 subregions of size 20' x 20', and assume that the mean height $\tilde{h}$ is constant within each subregion, but changes from region to region (a sufficiently justified assumption as shown in the next chapter); assume furthermore that dense gravity material is available in the whole region. Under these assumptions we plot the free-air anomalies versus height for each sub-region and should expect a correlation behavior which shows a parallel shift from one sub-region to the next as illustrated in Figure 3.1 below.

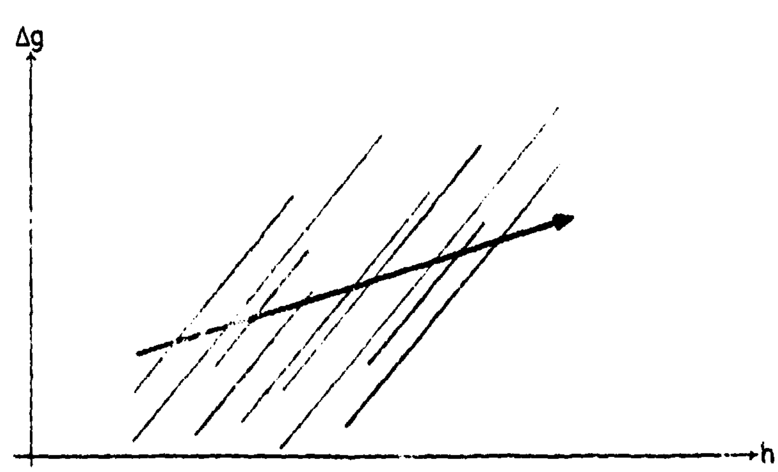

Fig. 3.1 Correlation model between free-air anomaly and topographic height.

(note that the parallel shift is due to the different mean heights.) If we perform a least-squares adjustment solution for the estimation of the parameter b for the whole region, we will get a too small value $\hat{b}$ which is indicated by the direction of the boldface arrow in Fig. 3.1. The reasoning is very simple: the parallel shift is essentially the signal s; in the adjustment procedure this signal is treated as random noise; with other words, the adjustment solution is blind with respect to horizontal position, it simply makes a mishmash of Δg with respect to h and not of its gradient as it should.

In contrast to the adjustment solution, the least-squares collocation solution takes care of the signal very carefully; it uses all the information contained in s, provided in terms of covariances, in order to estimate a) a common gradient b and b) the signal field as such (equ. (3.9), (3.10)). Therefore, a regional collocation solution will significantly improve the estimation of b as compared to a regional adjustment solution whenever a) the region is large, and b) the terrain is not flat.

It should be mentioned that Uotila (1967a,b) performed extensive numerical studies in order to find an optimal procedure for the estimation of a regionally valid parameter b. He finally came to the conclusion that a resonable estimate can, in general, only be achieved if the region is subdivided into smaller subblocks; for each subblock a local parameter b should be estimated by least-squares adjustment, the regional value is obtained as an appropriate average of all local b - values. His conclusions are in favorable agreement with ours; here a simple explanation of this phenomenon has been provided. A mathematically sound reasoning will be attempted in chapter 4.

Let us turn back to the signal and its statistical behavior. The collocation estimation of the parameter vector (3.9) requires the knowledge of the signal's covariance function which we do not necessarily have at hand; however, if a sufficiently large number of data is available within the considered region, we can proceed iteratively: we chose the standard value $b = 0.112$ as starting parameter, obtain the signal at the data points by

$$s_P \doteq \Delta g_P - M\{\Delta g\} - b_0 (h_P - M\{h\}), \tag{3.20}$$

calculate an empirical covariance function. and fit an appropriate model covariance function which is used in the estimation of the parameter vector. If necessary (hardly ever it is) we can determine better estimates of the signal and so forth. By far the most expensive part in the least-squares collocation solution remains the calculation of the individual covariances and the inversion of the covariance matrix.

The least-squares collocation solution presented here was based on the very essential and restricting assumption that free-air anomalies and elevations are linearly correlated; in other words, we have assumed that the covariance functions $\text{cov}(\Delta g^r, h^r)$ and $\text{cov}(h^r, h^r)$ are proportional for all arguments, a condition which was imposed in order to render the signal s independent of elevation. However, if this condition is intolerably violated, a more general approach has to be aimed at. In a very early paper Moritz (1963) has laid down the basic formulas which express the optimally predicted centered free-air anomaly in terms of a linear combination of centered free-air anomalies and centered elevations. The predicted quantity is given by the familiar expression

$$\Delta g_P^r = C_P^T C^{-1} \ell^r \quad . \tag{3.21}$$

In this context ℓ denotes the vector

$$\ell^T = (\Delta g_1^r , \Delta g_2^r , \ldots, \Delta g_n^r , h_1^r , h_2^r , \ldots, h_n^r , h_P^r);$$

note that the elevation h_P^r of the prediction point is an element of the "data" vector. This peculiar case deserves some attention: the free-air anomaly is a function of horizontal and vertical position; its restriction to the surface of the earth is characterized by (2.3). A linear predictor has to represent Δg in terms of

$$\Delta g_P^r = \alpha_P^T \Delta g^r + \beta_P^T h^r + \gamma_P h_P^r \tag{3.22}$$

with coefficients α_P^T, β_P^T and γ_P independent of elevation. Since h^r is correlated with Δg^r, the minimization of the prediction error leads to a linear system which consists of covariances between data (usual case) <u>and</u> covariances between the elevation at the prediction point and all data. Therefore, we obtain a covariance matrix which can be partitioned into 4 blocks,

$$C = \begin{bmatrix} C_1 & C_2 \\ C_2^T & C_3 \end{bmatrix}$$

with the prediction-point-independent (data, data) - covariance matrix C_1 and the variance of centered heights C_3, and the prediction-point-dependent block C_2 which is a vector of covariances between the height at the prediction point and all data. When we are talking about "data", we have the set

$$(\Delta g_1^r , \Delta g_2^r , \ldots, \Delta g_n^r ; h_1^r , h_2^r , \ldots, h_n^r)$$

in mind.

Here we see already the drawback of this general and optimal prediction method:

A) We need to know

a) the autocovariance function of free-air anomalies $\mathrm{cov}(\Delta g^r, \Delta g^r)$,

b) the autocovariance function of the topography $\mathrm{cov}\,(h^r, h^r)$,

c) the crosscovariance function of free-air anomaly and topography;

B) Each prediction requires the calculation and inversion of a covariance matrix which, in contrast to usual least-squares prediction problems, changes with the horizontal position of the prediction point; (the covariance matrix is invariant with respect to the vertical position of the prediction point only, but not with respect to its horizontal position.)

As a matter of fact, this peculiar property of the covariance matrix makes predictions more expensive, however, not as much as one would expect from a first glance, for the following reason: the block C_1 is invariant with respect to the location of the prediction point and, therefore, C_1 has to be inverted only once and for all. The remaining parts of the inverse covariance matrix can be obtained by a simple block-partitioning (cf. Faddeeva, 1959, § 14):

$$C^{-1} = \begin{bmatrix} C_1 & C_2 \\ C_2^T & C_3 \end{bmatrix}^{-1} = \begin{bmatrix} B_1 & B_2 \\ B_2^T & B_3 \end{bmatrix}$$

with

$$B_3 = 1/(C_3 - C_2^T C_1^{-1} C_2)^{-1} \qquad (3.23)$$

$$B_2 = - C_1^{-1} C_2 B_3$$

$$B_1 = C_1^{-1} + B_2 B_2^T / B_3 \quad .$$

Assuming n data given (1 data consists of Δg^r and the corresponding h^r), C_1 has dimension 2n x 2n, C_2 has dimension 2n x 1, and C_3 is a constant. Observing (3.23) we conclude that on the order of $8n^2$ basic operations (multiplication + addition) are required for the calculation of the full inverse covariance matrix provided that C_1^{-1} is already available. In view of the fact that the calculation of C_1^{-1} requires on the order of $8n^3$ basic operations, we conclude that the prediction of n anomalies is just twice as expensive as the calculation of C_1^{-1} (which is approximately equal to the prediction of a single point anomaly). Therefore, the dependence of the covariance matrix on the horizontal location of the prediction point will not blow up the computation time too much and cannot be considered a severe limitation. There are much stronger arguments which do not speak in favor of this "optimal" solution.

Let us compare the collocation solution, which assumes linear correlation between Δg and h, with the collocation solution based on a rather arbitrary correlation behavior. The solution (3.10) requires the estimation of a single covariance function, its fit by an appropriate model, the calculation of about $n^2/2$ covariances, and the inversion of a n x n symmetric and positive definite matrix if n gravity anomalies are processed. The general method requires the estimation of 3 times more covariance functions, their fit by appropriate models, the calculation of about 4 times more covariances and 8 times more basic operations for the calculation of the inverse covariance matrix. Therefore, it seems to be on the order of 5 times more expensive than the collocation solution based on the linear correlation model. Particularly troublesome seems to be the estimation of $\mathrm{cov}(\Delta g^r, h^r)$ and $\mathrm{cov}(h^r, h^r)$ because

of the generally lacking data density, particularly in mountainous areas, where there would be a real need for. For these reasons, it is rather questionable if the optimal solution for the general case differs significantly from the linear correlation solution (if a linear correlation exists, both solutions are identical), and if a small improvement of the solution justifies the very high price to be paid.

The following Table summarizes r m s - prediction errors of mean free-air anomalies, depending on the data density and the correlation length ξ of the covariance function; a variance of 100 $mgal^2$ has been used. The data are assumed to be regularly distributed error-free point gravity anomalies. A data density of N means N data/blocks.

The figures in Table 3.1 do not include the error introduced by the inaccuracies of the trend model parameters a and b; they can contribute to the total error budget up to 2 - 3 mgal (Sünkel and Malits, 1981); a typical error estimate of a is $\pm$ 1.5 mgal, a typical error estimate of b is $\pm$0.002 mgal/m. Note that the variance of 100 $mgal^2$ has been chosen rather arbitarily; the figures can easily be scaled by the proper variance.

correlation length ξ (km)

N	20	30	40	50	60	
1	0.5	0.3	0.2	0.10		$5' \times 5'$
4	0.1					
1	1.6	0.9	0.5	0.4	0.3	$10' \times 10'$
4	0.3	0.2	0.1			
1	2.6	1.6	1.1	0.7	0.5	$15' \times 15'$
4	0.5	0.3	0.2	0.2	0.1	
9	0.1					
1	3.8	3.2	2.6	2.0	1.6	$30' \times 30'$
4	1.4	0.8	0.5	0.3	0.3	
9	0.5	0.2	0.1			
16	0.2	0.1				
1	3.6	3.9	3.8	3.6	3.2	$1^{\circ} \times 1^{\circ}$
4	2.4	1.9	1.4	1.0	0.8	
9	1.3	0.8	0.5	0.3	0.2	
16	0.7	0.3	0.2	0.1	0.1	
25	0.4	0.2	0.1			

Table 3.1 Mean free-air anomaly r m s - prediction errors (mgal), depending on the data density N (= number of data/block) and on the correlation length ξ; common variance: 100 $mgal^2$.

The results summarized in Table 3.1 are graphically represented in Fig. 3.2 a-e. The contours are lines of constant mean free-air anomaly prediction error dependent upon the correlation length ξ (horizontal axis) and the data density (vertical axis). Note that these estimates refer to the ideal situation of regularly distributed and error-free data having a variance of 100 mgal^2;

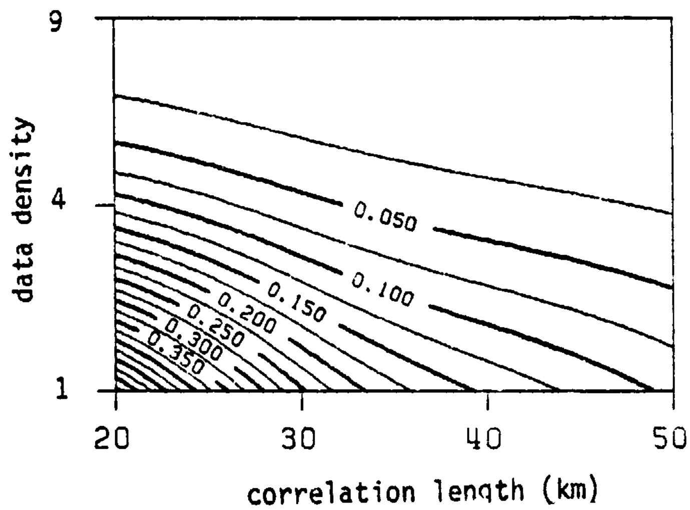

(a) 5´ x 5´

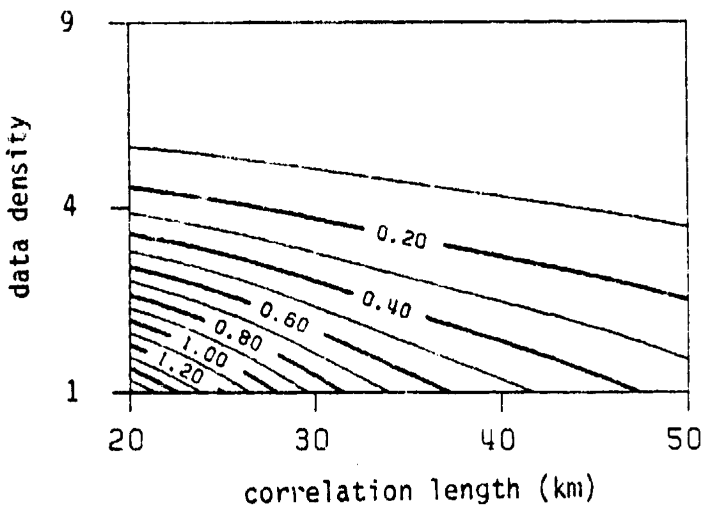

(b) 10´ x 10´

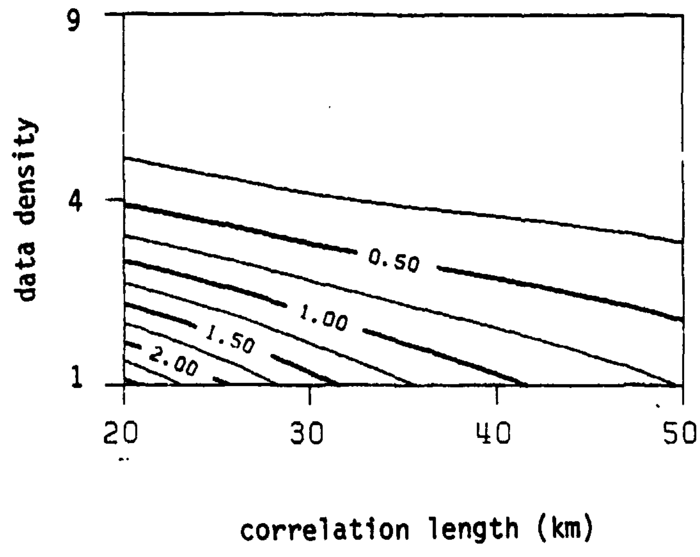

(c) 15′ x 15′

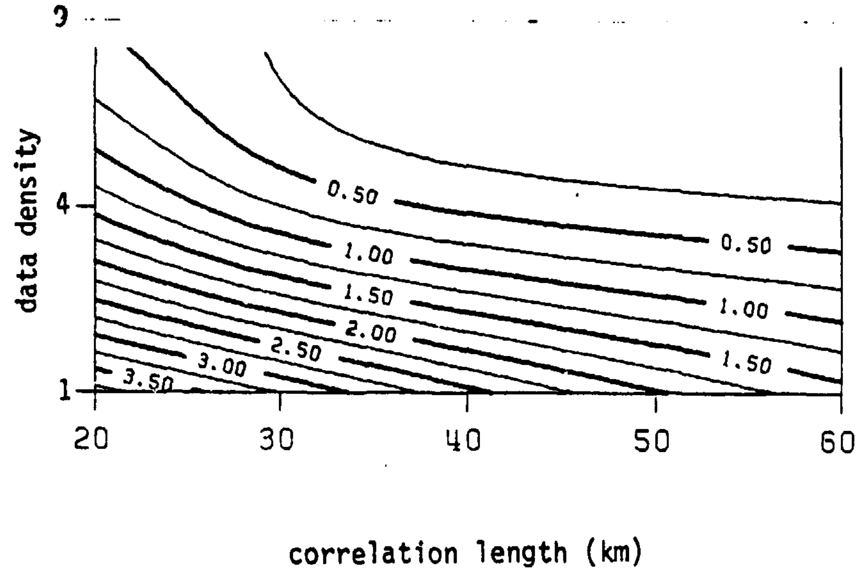

(d) 30′ x 30′

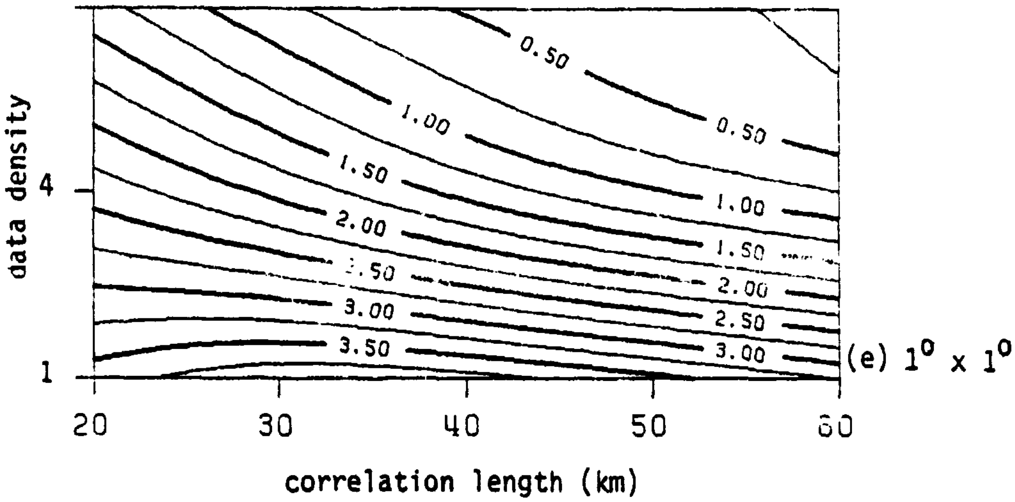

Fig. 3.2 a-e Lines of constant rms mean anomaly prediction error, depending on the correlation length and the data density; variance: 100 mgal²

As a matter of fact the estimates obtained here have to be scaled according to the individual variance. The variance can considerably differ between various areas; this is why, as a kind of normalizing factor, a common 100 mgal² variance has been assumed. E.g. the mean residual variance for a $1^{\circ} \times 1^{\circ}$ area is of the order of 900 mgal² (total variance minus variance of $1^{\circ} \times 1^{\circ}$ mean anomalies); therefore, the values of Fig. 3.2e should (in average) be multiplied by a factor 3. All values refer to the covariance model of Hirvonen $C(s) = C_0/[1+(s/\xi)^2]$; for the Gaussian covariance model $C(s) = C_0 e^{-a^2 s^2}$ we obtained estimates which are about 50% lower for $5' \times 5'$ mean values and 15% lower for $1^{\circ} \times 1^{\circ}$; these lower estimates are due to the stronger correlation of the Gaussian model, compared to the Hirvonen model, for small distances; the covariance function's behavior for small distances is controlled by its curvature parameter at the origin; therefore, highly reliable prediction and prediction error estimates should be based on a covariance model which resembles all three essential parameters, the variance, the correlation length and the variance of horizontal gradients.

4. The b = const. - PROBLEM and ISOSTASY

In chapter 3 basically three methods for the prediction of free-air anomalies have been presented. Two of them assumed a linear correlation between free-air anomalies and elevations, represented by the correlation coefficient b. In least-squares adjustment determinations of b (equ. (3.8)′) , it has been observed (Uotila, 1967 a,b) that $|b|$ tends to decrease if the area, for which it is considered constant, increases. A simple explanation of this phenomenon has been provided; it was based on the assumption that the value of the Bouguer anomaly is approximately proportional to a "mean" height. It has been anticipated that the way of taking the mean of the topography is closely linked to the concept of isostasy. In this chapter we make the attempt to obtain a mathematical relation between the area size (of b considered constant), statistical characteristics of the topography, and the error to be expected in b due to the b = const. assumption.

Moritz (1969) has shown by means of a simplified model of isostasy, that the linear correlation between free-air anomalies and topographic elevations can be explained in a very simple way. Representing the compensated masses by a surface layer at the depth D below sea level, he finally arrives, after some minor neglections, at a relation which expresses the free-air anomaly in terms of the corresponding point height, the corresponding mean height, and the topographic correction,

$$\Delta g_P = 2\pi G\rho\,(h_P - \tilde{h}_P) - C_P \;, \tag{4.1}$$

$\dot{h}_P$ ... elevation of the point

$\tilde{h}_P$ ... mean elevation corresponding to P,

C_P ... topographical correction,

ρ ... density,

G ... gravitational constant.

(Note that for this model the Bouguer anomalies are given by $-2\pi G\rho\tilde{h}_P$, the isostatic anomalies vanish.)

The mean height $\tilde{h}_P$ is represented in terms of the output of a linear system with input h,

$$\tilde{h}(P) = \frac{R^2 D}{2\pi} \iint_\sigma \frac{h(Q)}{\ell_c^3(P.Q)}\, d\sigma\,(Q) \tag{4.2}$$

with ℓ_c denoting the distance between the point P_0 (located at sea level, orthogonal projection of the surface point P) and Q (located on the compensation surface at depth D below sea level); R denotes the mean radius of the earth. In the spectral domain the mean height spectrum $\tilde{h}_{nm}$ is related to the point height spectrum h_{nm} through

$$\tilde{h}_{nm} = \kappa_n h_{nm} , \tag{4.3}$$

where κ_n is the n'th degree eigenvalue of the integral kernel K of (4.2),

$$K(P.Q): = \frac{R^2 D}{2\pi} \frac{1}{\ell_c^3\,(P.Q)} . \tag{4.4}$$

According to the Funck-Hecke formula (Müller, 1966, p. 20),

$$\kappa_n = 2\pi \int_{-1}^{1} K(t) P_n\,(t)dt; \tag{4.5}$$

(P_n is the Legendre polynomial of degree n.) Introducing (4.4) in (4.5), κ_n is expressed by

$$\kappa_n = R^2 D \int_{-1}^{1} \frac{P_n(t)}{\ell_e^3(t)}\, dt \,. \qquad (4.5)'$$

ℓ_e as the distance between P_0 and Q is given by

$$\ell_e = \left[R^2 + (R-D)^2 - 2R\,(R-D)\cos\psi\right]^{\frac{1}{2}},$$

and $1/\ell_e^3$ by

$$\frac{1}{\ell_e^3} = \frac{1}{R^3}\,(1 + \alpha^2 - 2\alpha t)^{-\frac{3}{2}} \qquad (4.6a)$$

with $\quad \alpha : = 1 - \frac{D}{R}\,, \; t : = \cos\psi \,. \qquad (4.6b)$

The expression (4.6a) can be represented in terms of a series of Legendre polynomials (Heiskanen & Moritz, 1967, p. 35),

$$\frac{1}{\ell_e^3} = \frac{1}{R^3(1-\alpha^2)} \sum_{n=0}^{\infty} (2n+1)\,\alpha^n\; P_n\,(\cos\psi)\;. \qquad (4.7)$$

Now it is fairly easy to derive the eigenvalues κ_n; observing the orthogonality relation of Legendre polynomials expressed through

$$\int_{-1}^{1} P_n\,(t)\, P_m\,(t)\, dt = \frac{2}{2n+1}\,\delta_{nm}$$

(δ_{nm} denotes the Kronecker symbol), we obtain with (4.5) and (4.7)

$$\kappa_n = \frac{2\alpha^n}{(1+\alpha)} \;; \qquad (4.8)$$

expressing α by (4.6b) we obtain

$$\kappa_n = \frac{(1-\frac{D}{R})^n}{(1-\frac{D}{2R})} \quad . \qquad (4.8)'$$

In order to better understand the impact of these eigenvalues, let us consider two extreme cases:

a) D = 0 (compensation level coincides with sea level): in this case both the isostatic and the Bouguer anomalies should be identically zero according to our model (4.1). In other words, $\tilde{h} \equiv h$ - no smoothing is envolved. In terms of the spectrum this means that $\tilde{h}_{nm} = h_{nm}$, therefore all κ_n must be identically 1. This condition is obviously fulfilled by the eigenvalues (4.8)′.

b) D = R (compensation "level" coincides with the center of the sphere): in this case the isostatic compensation degenerates, such that the mean height becomes independent on point position and, therefore, a constant. As a consequence only the zero degree eigenvalue has to be equal to one (it passes the operator undisturbed), all other eigenvalues must be zero (annihilation of all frequencies higher than zero). This condition is also fulfilled by the eigenvalues (4.8)′.

In other words, (a) represents an extreme case of a high-pass filter, (b) an extreme case of a low-pass filter. Our isostatic model as well as the actual isostatic compensation will be located somewhere in between (a) and (b). The following graph presents the behavior of the eigenvalues κ_n for three generally discussed and used compensation depths, D = 24, 32, and 40 km.

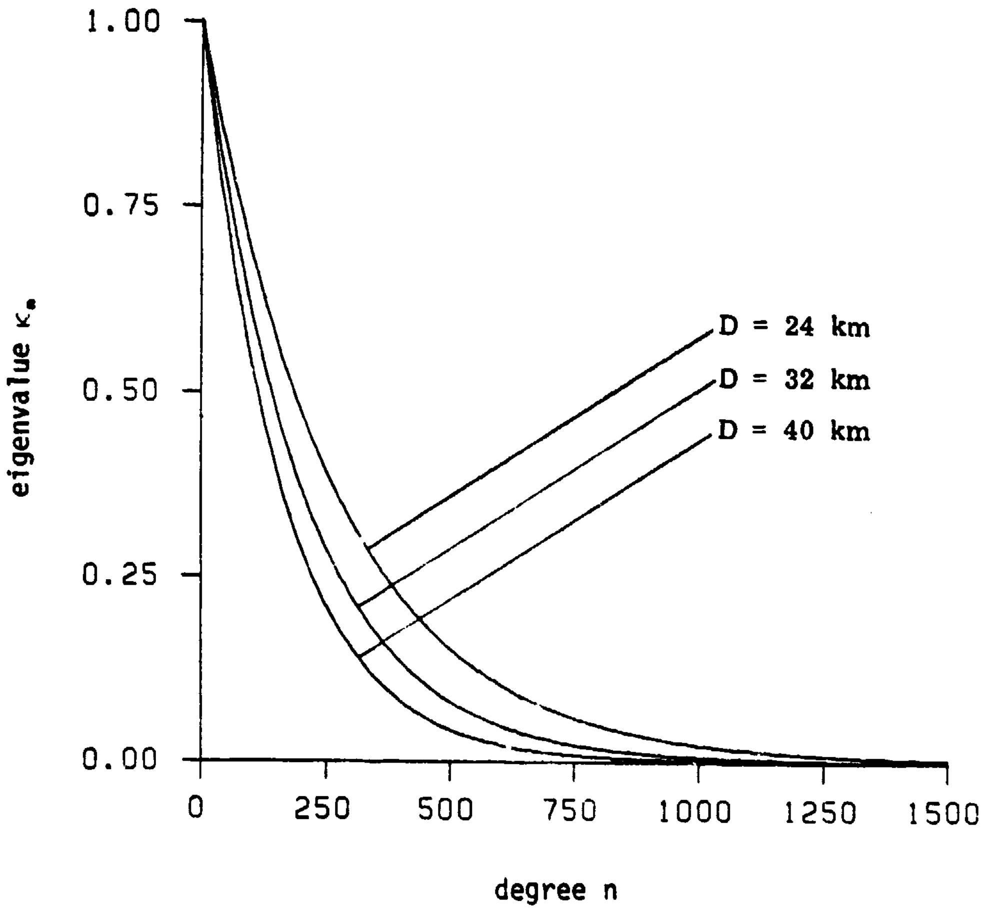

Fig. 4.1 Eigenvalues κ_n of topography - smoothing operator.

Let now the topography be given in terms of a series of normalized harmonics ϕ_{nm},

$$h(P) = \sum_{n,m} h_{nm}\, \phi_{nm}\,(P), \tag{4.9a}$$

then the corresponding smoothed topography is obtained through

$$\tilde{h}(P) = \sum_{n,m} \kappa_n h_{nm}\, \phi_{nm}(P) \tag{4.9b}$$

and the residual topography $\Delta h = h - \tilde{h}$

$$\Delta h(P) = \sum_{n,m} (1-\kappa_n) h_{nm}\, \phi_{nm}(P). \tag{4.9c}$$

The corresponding autocovariance functions of h, $\tilde{h}$, and Δh are given by

$$\mathrm{cov}(h,h) = \sum_{n>0,m} h_n\, P_n\,(\cos\psi) \tag{4.10a}$$

$$\mathrm{cov}(\tilde{h},\tilde{h}) = \sum_{n>0,m} \kappa_n^2\, h_n P_n\,(\cos\psi) \tag{4.10b}$$

$$\mathrm{cov}(\Delta h,\Delta h) = \sum_{n>0,m} (1-\kappa_n)^2 h_n P_n\,(\cos\psi) \tag{4.10c}$$

with the degree variances $h_n = \sum_{m=-n}^{n} h^2{}_{nm}$.

The behavior of $(1-\kappa_n)^2$ for three compensation depths is shown in Fig. 4.2. The energy in the low frequency part is dampened because the low frequency content of h and $\tilde{h}$ is almost the same. The energy in the high frequencies, however, is hardly reduced since $\tilde{h}$ has hardly any power in the high frequencies. The deeper the compensation level, the more energy remains from the high frequent part.

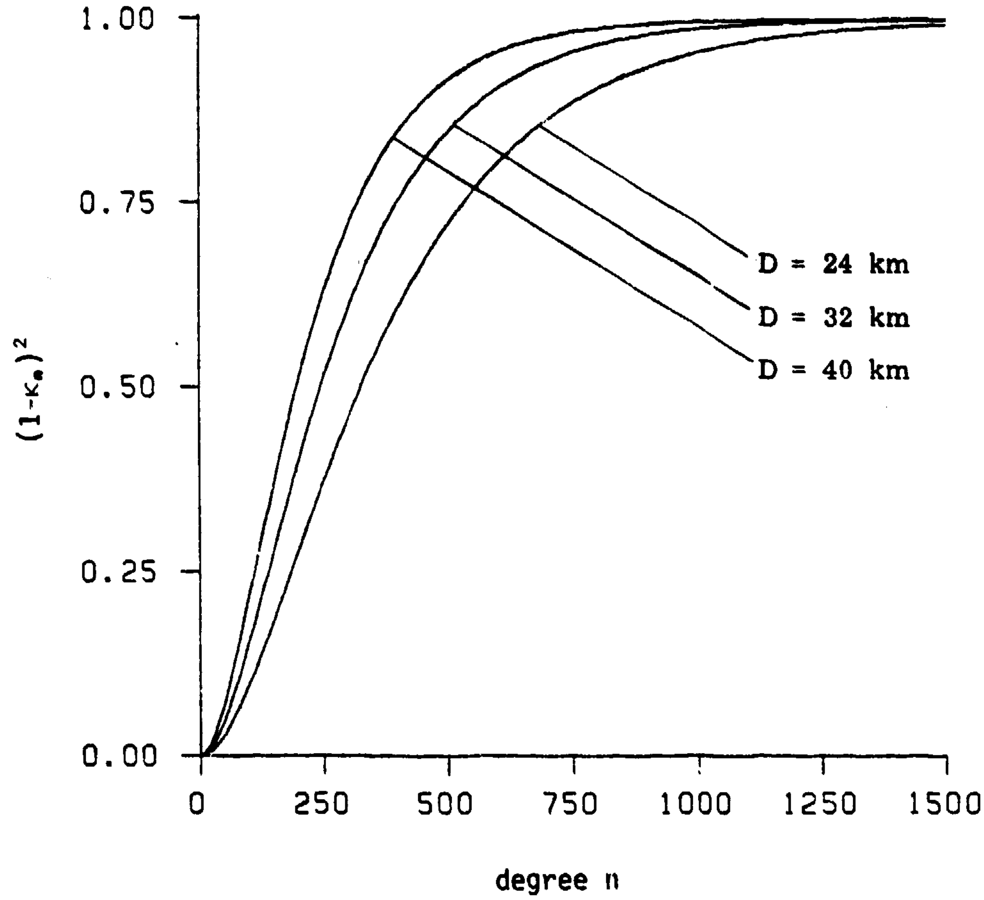

Fig. 4.2 Energy dampening factor for residual height.

What we are primarily concerned about, is the b = const. - problem. Considering again the ideal case of homogeneous density and terrain-corrected free-air anomalies, we conclude from the model (4.1) that b is constant if the mean height, as defined by (4 2), is used. However, in practical determinations of b, valid for a specific area, a <u>constant</u> mean height is used. In gneral, $\tilde{h}$ as defined by (4.2) is not constant over a limited area such as $1^{o} \times 1^{o}$. The error which we commit by using a constant mean height instead of a variable mean height $\tilde{h}$ enters

fully in the determination of b. Denoting the constant height of a specific region by $\bar{h}$ and $2\pi G\rho$ by b_0, the factor b, as determined by a least-squares adjustment (equ. (3.8)'), is obtained by

$$\hat{b} = \frac{h'^T \Delta g'}{h'^T \; h'} \quad , \tag{4.11}$$

where h' and $\Delta g'$ denote the vectors of residual elevation and (terrain corrected) free-air anomalies,

$$h'^T : = (h_1-\bar{h}, h_2-\bar{h}, \ldots, h_n-\bar{h}),$$

$$\Delta g' : = (\Delta g_1-\overline{\Delta g}, \Delta g_2-\overline{\Delta g}, \ldots, \Delta g_n-\overline{\Delta g}).$$

According to our assumption, the mean anomaly $\overline{\Delta g}$ is given by

$$\overline{\Delta g} = b_0 \; (\bar{h} - \bar{\tilde{h}}) \tag{4.12}$$

and therefore, the reduced anomalies can be represented by

$$\begin{aligned} \Delta g' &= b_0(h - \tilde{h}) - b_0(\bar{h} - \bar{\tilde{h}}) \\ &= b_0(h - \bar{h}) - b_0(\tilde{h} - \bar{\tilde{h}}) \\ &= b_0 \; h' - b_0 \tilde{h}' \quad . \end{aligned} \tag{4.13}$$

Introducing this relation into (4.11), the error $\delta b : = \hat{b} - b_0$ is given by

$$\delta b = b_0 \frac{h'^T \tilde{h}'}{h'^T h'} \; ,$$

and, with the triangle inequality $|a\, b| \leq |a|\,|b|$, we obtain an estimate

$$|\delta b| \leq b_0 \; \frac{|\tilde{h}'|}{|h'|} \quad . \tag{4.14}$$

From (4.13) it is obvious that the error δb vanishes if the size of the area, for which $\bar{h}$ and $\overline{\Delta g}$ are constant, goes to zero. Vice versa, δb will increase with increasing area size. Equation (4.14) shows that δb is proportional to the r m s variation of the residual mean elevation as defined by (4.2), and indirect proportional to the r m s variation of the residual elevation. Therefore, an estimate of b for small blocks in mountainous areas should give small estimation errors, provided our model is correct and the data distribution is sufficiently homogeneous and dense. Poor estimates have to be expected for large blocks in flat areas. Both phenomena have been strongly confirmed by practical determinations of b (Uotila, 1967a,b; Sünkel and Malits, 1981).

The mean elevation $\tilde{h}$ is defined as a weighted average of the elevation h with distance-dependent weights; $\tilde{h}(\cdot)$ is a smooth surface. This smooth surface, however, is approximated by a step function $\bar{h}$ in all practical applications. As we have seen above, the variation of $\tilde{h}$ with respect to a constant is responsible for the error in δb, provided our model is valid; the block size is closely related to the error δb. Since we shall hardly ever work with a mean surface $\tilde{h}$ but rather with $\bar{h}$ we are interested in the effect of δb, caused by the replacement of $\tilde{h}$ by h. We will again consider Faye - anomalies (terrain corrected free-air anomalies) which are linearly related to the elevation h,

$$\Delta g = b_0(h - \tilde{h}) \; ;$$

if we replace h by $\bar{h}$, we make b variable (b_0 is a global constant) and dependent on position,

$$\Delta g = b\,(h - \bar{h}) \; .$$

The right hand sides of both equations have to be equal for all points, and we obtain the condition

$$b_0(h - \tilde{h}) = b(h - \bar{h}). \tag{4.15}$$

Splitting b up into $b = b_0 - \delta b$ and adding zero to the right hand side, we obtain

$$b_0(h - \tilde{h}) = (b_0 - \delta b)(h - \tilde{h} + \tilde{h} - \bar{h}),$$

and consequently

$$\delta b(h - \bar{h}) = b_0(\tilde{h} - \bar{h}). \tag{4.15'}$$

(Note that δb, h, $\tilde{h}$ are variable, $\bar{h}$ is constant.) If b is determined by means of least-squares adjustment with parameters, the function $\delta b(h - \bar{h})$ is considered as noise; in our model this noise is represented by the difference between the mean elevation surface $\tilde{h}$ and the constant $\bar{h}$. Note that in the least-squares collocation solution $b_0(\tilde{h} - \bar{h})$ is treated as a signal, but not as noise. As a matter of fact, the power of this noise is a measure for the error of estimation of b in the least-squares adjustment concept.

In the sequel we shall investigate the average deviation of $\bar{h}$ from $\tilde{h}$. The derivations are particularly simplified if $\bar{h}$ is considered as the mean elevation over a circular region and, moreover, if $\bar{h}$ is considered as the output of a moving average applied to the actual topography h. These two simplifying assumptions do not quite reflect reality, but the advantage of working with the concept of isotropy justifies this formal inaccuracy.

The moving average $\bar{h}$ of h, taken over a circular cap with radius ψ_0, can be expressed by

$$\bar{h}(P) = \sum_{n,m} \beta_n h_{nm} \phi_{nm}(P) \tag{4.16}$$

for the same reason and in the same way as $\tilde{h}$ was exp·essed by (4.9b). In this context β_n are the eigenvalues of an isotropic moving average operator with an integral kernel $B(t;\, t_0)$ defined by

$$B(t) = \begin{cases} \dfrac{1}{2\pi(1-t_0)} & \text{for } t_0 \leq t \leq 1 \\ 0 & \text{else} \end{cases} \quad . \tag{4.17}$$

(t denotes the cosine of the spherical distance.) The eigenvalues are obtained through

$$\beta_n(t_0) = \frac{1}{1-t_0} \int_{t_0}^{1} P_n(t)\, dt.$$

The following expression can be found in (Meissl, 1971, p. 24):

$$\beta_n(t_0) = \frac{1}{1-t_0} \, \frac{1}{2n+1} \left[P_{n-1}(t_0) - P_{n+1}(t_0) \right] ; \tag{4.18a}$$

Sjöberg (1980) has recently derived a quite attractive recurrence relation which does not require the computation of the Legendre polynomials:

$$\beta_n(t_0) = \frac{1}{n+1} \left[(2n-1)t_0\beta_{n-1}(t_0) - (n-2)\beta_{n-2}(t_0) \right], \; n \geq 2$$

with $\quad \beta_0 = 1 \;$ and $\; \beta_1(t_0) = \frac{1}{2}(1+t_0)$. (4.18b)

With (4.9b) and (4.16), the relative error $\delta b/b_0$ (equ. (4.15)') can be represented by

$$\frac{\delta b(P)}{b_0} = \frac{\sum_{n,m} (\kappa_n - \beta_n) h_{nm} \phi_{nm}(P)}{\sum_{n,m} (1-\beta_n) h_{nm} \phi_{nm}(P)} \quad . \tag{4.15}$$

It is obvious that δb vanishes if $\kappa_n = \beta_n$ for all n. Due to the different behavior of κ_n and β_n, this condition is only fulfilled in the extreme cases of

a) $D = 0$ and $\psi_0 = 0$,

b) $D = R$ and $\psi_0 = \pi$.

For all other realistic situations like D=24, 32, or 40 km as discussed here, β_n will in general be different from κ_n; therefore, b will not vanish. The variance of

$$\sum_{n,m} (\kappa_n - \beta_n) h_{nm} \; \phi_{nm}(P),$$

given by $\sum_n (\kappa_n - \beta_n)^2 h_n$ (4.19)

is obviously a measure for the mean square value of δb. Therefore, the goal is to minimize (4.19) which can be achieved by selecting, for each compensation depths D, an appropriate cap radius ψ_0. However, the optimal relation between D and ψ_0 is influenced by the actual degree variances of the topography. This means that we have to know the degree variances h_n of the topography. Rapp (1981) has recently determined the degree variances of rock topography for $n \leq 180$ based on a $1^\circ \times 1^\circ$ mean elevation data set. They can be used in (4.16) to represent the energy which is contained in the long-to-medium wavelengths of the topography. Higher degree variances have to be obtained from a degree variance model. Since the author is not aware of the existence of an appropriate model,

another way has been chosen: In the medium frequency range the actually "observed" free-air gravity anomaly degree variances and the corresponding ones derived from topographic data agree fairly well; this agreement should be even better in the high frequency range because of the strong linear correlation between gravity and elevation. Therefore, it was quite natural to use this source of information as topographical height degree variance model for medium to high frequencies.

Two gravity anomaly degree variance models which fit real world gravity data best (potential coefficients to degree 180 based on a complete set of $1^{o} \times 1^{o}$ mean free-air anomalies, an observed variance of 1800 $mgal^2$, and a variance of the horizontal gravity gradient of 800 E^2), are two parameter models suggested by Moritz (1977), numerically investigated by Jekeli (1978) and Rapp (1979). Both models have the form

$$C_n = (n-1)\left[\frac{\alpha_1 \sigma_1^{n+2}}{n+A_1} + \frac{\alpha_2\ \sigma_2^{n+2}}{(n-2)(n+A_2)}\right] \tag{4.20}$$

and are determined by 6 parameters each. "Case One" model of Rapp (1979) gives the best overall fit to the data, "Case Two" model fits the observed degree variances best.

model	α_1[$mgal^2$]	α_2[$mgal^2$]	σ_1	σ_2	A_1	A_2
"Case One"	3.4050	140.03	.998006	.914232	1	2
"Case Two"	14.966	999.25	.987969	.850000	75	20

Table 4.1 Used "best" degree variance model parameters, from Rapp (1979), p. 15.

For a linear correlation model between gravity and elevation with the Bouguer-factor $2\pi G\rho$ = 0.112 mgal/m, the relation between the degree variances h_n (elevation) and c_n (gravity) is given by

$$h_n = \frac{c_n}{(2\pi G\rho)^2(1-\kappa_n)^2} \quad . \tag{4.21}$$

Figures 4.3a,b show the degree variances of observed rock topography up to degree 180, and such ones derived from Rapp's "Case One & Two" gravity anomaly degree variance models for n>180.

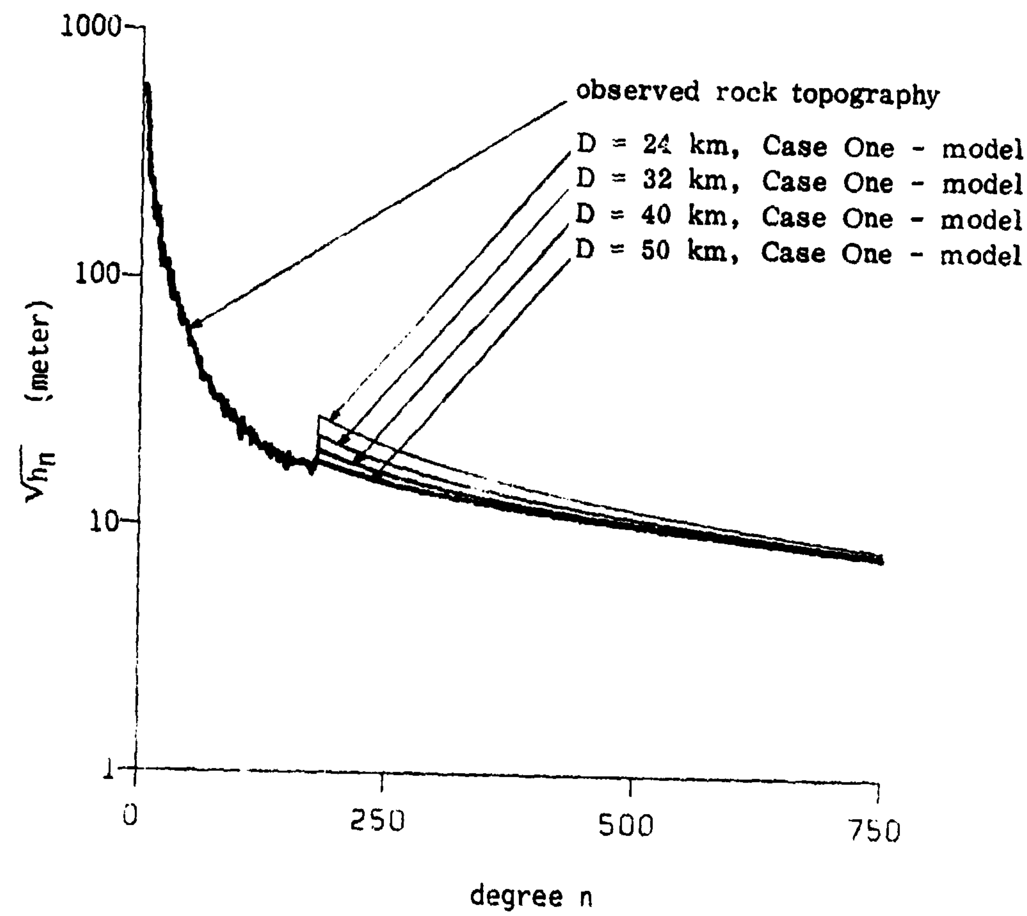

Fig. 4.3a Observed ($n \leq 180$) and from (4.20) and (4.21) derived (n>180) rock topography degree variances ("Case One" - model) based on various compensation depths.

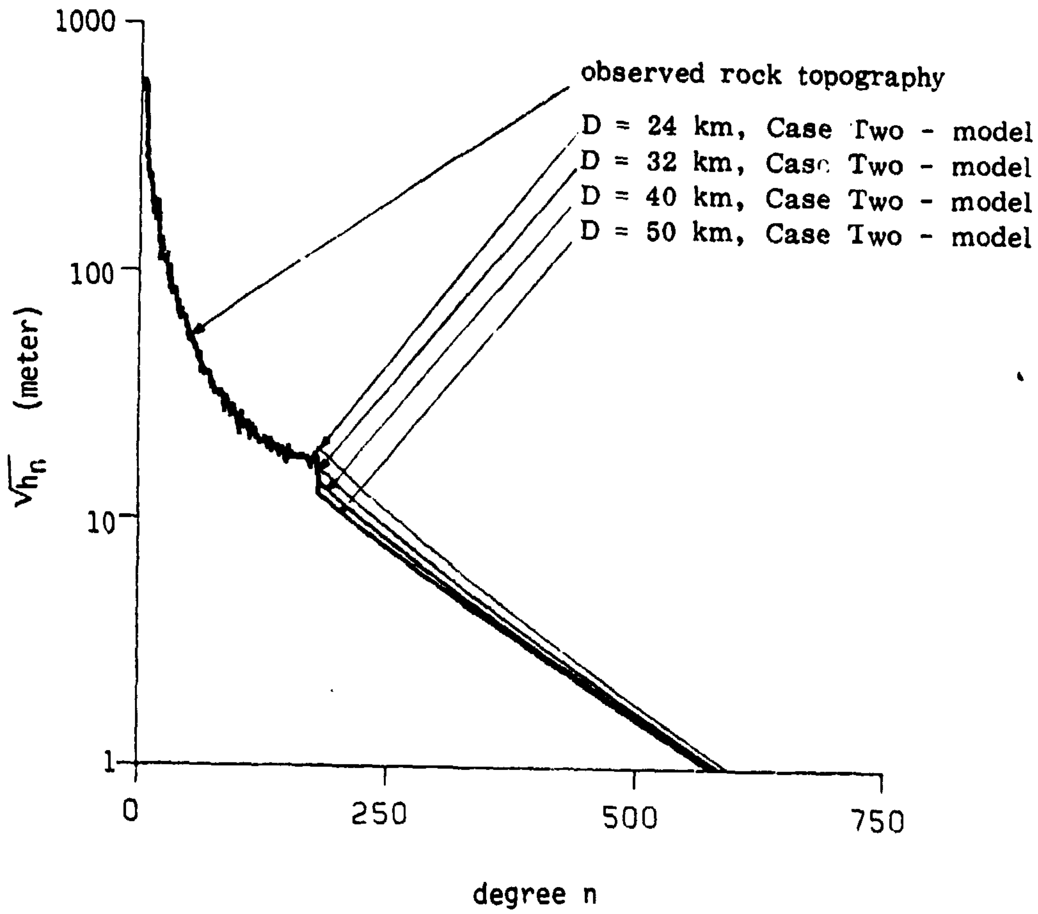

Fig. 4.3b Observed ($n \leq 180$) and from (4.20) and (4.21) derived ($n>180$) rock topography degree variances ("Case Two"-model) based on various compensation depths.

It is obvious from the above two figures that the "Case Two"-model has much less power in the high frequency part than the "Case One"-model. "Case One"-model matches the trend obviously much better; the 50 km compensation depths seems to be optimal for the "Case One" model, 32 km for the "Case Two"-model.

The contribution of each degree variance to (4.19) is weighted by $(\kappa_n-\beta_n)^2$. These weights are graphically represented in Figures 4.4a-c for various compensation depths and cap sizes. Needless to say, the zero line corresponds to the never fulfilled ideal case $\kappa_n = \beta_n, \forall n$. The following conclusions can be drawn from these figures: The weights depend strongly on the assumed compensation depth; for the cases considered here (D=24,32, and 40 km), the cape sizes ψ_0=15′ and ψ_0=2° can be ruled out because of their too large deviation from the ideal case; for the generally adopted compensation depth D=32 km the overall weight minimum is somewhere around ψ_0=30′ to 60′. The weights are significantly different from zero, up to degree n=750 which corresponds to a wavelength of about 50 km; high-frequent variations (n>750) of the topography are obviously very similarly averaged by (4.2) and (4.17); very low-frequent variations (n<36) are similarly averaged by (4.2) and (4.17) alike; the difference between κ_n and β_n is strongest in the medium-frequency range.

Since (4.16) does not only depend on κ_n and β_n but also on h_n, it is particularly important to have a good estimate for medium-degree rock topography degree variances available. Observed rock topography degree variances up to degree 180 were available to the autho·; due to the excellent correspondence between observed and anoma·y-derived degree variances for n ≈ 120 to 180, particularly for the "Case One"-model of Rapp (1979), it was decided to use this model as a representative one for de_ ees n>180. With this data we computed first the L_2-norm of

$$b_0 \| \tilde{h} - \bar{h} \| = | \langle \delta b, h - \bar{h} \rangle | \tag{4.22}$$

with $$\| f \|^2 := \frac{1}{4\pi} \iint_\sigma f^2 \, d\sigma ,$$

for various compensation depths D and cap radii ψ_0. Naturally, the norm depends on D as well as on ψ_0; for the optimal choice of ψ_0, corresponding to a prescribed D, the norm depends strongly on ψ_0, but weakly on D, and assumes values between 8 and 11 mgal; (this corresponds to a minimum r m s difference between $\tilde{h}$ and $\bar{h}$ of some 70 to 100 meters.) The 8 mgal value has been obtained for D=24 km, the "Case Two"- model and a cap radius of ψ_0=45´. Due to Schwarz´ inequality we are able to estimate a globally valid lower bound of the error δb through

$$\| \delta b \| \geq b_0 \frac{\| \tilde{h} - \bar{h} \|}{\| h - \bar{h} \|} \quad . \tag{4.23}$$

For the optimal choice of ψ_0, corresponding to a prescribed compensation depth D, the lower bound of $\| \delta b \|$ is practically constant and equals $3.0 \cdot 10^{-2}$ which is 30% of the normal Bouguer factor. Those optimal values have been obtained for D=24 km, ψ_0=40´ down to D=40 km, ψ_0=110´ and the

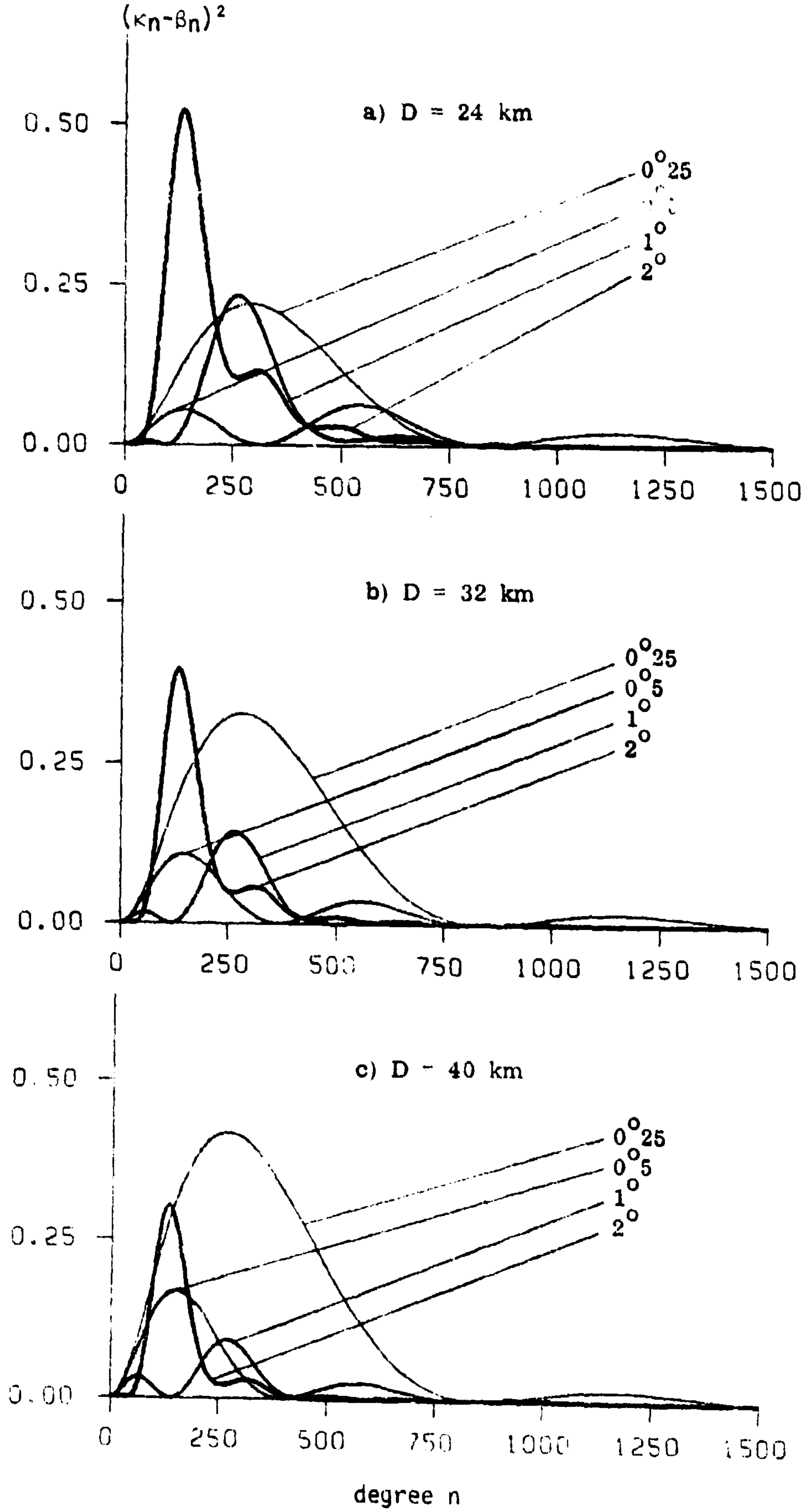

Fig. 4.4(a-c) Weights per degree for various compensation depths D and various choices of the cap size (radius ψ_0=0°25, ..., 2°)

"Case One"- model. The graphs in Figs. 4.5 and 4.6 show $b_0 \| \tilde{h}-\bar{h} \|$ and $\| \delta b \|$ as defined by (4.23) dependent on various compensation depths and cap sizes, for both the "Case One" and the "Case Two" - model.

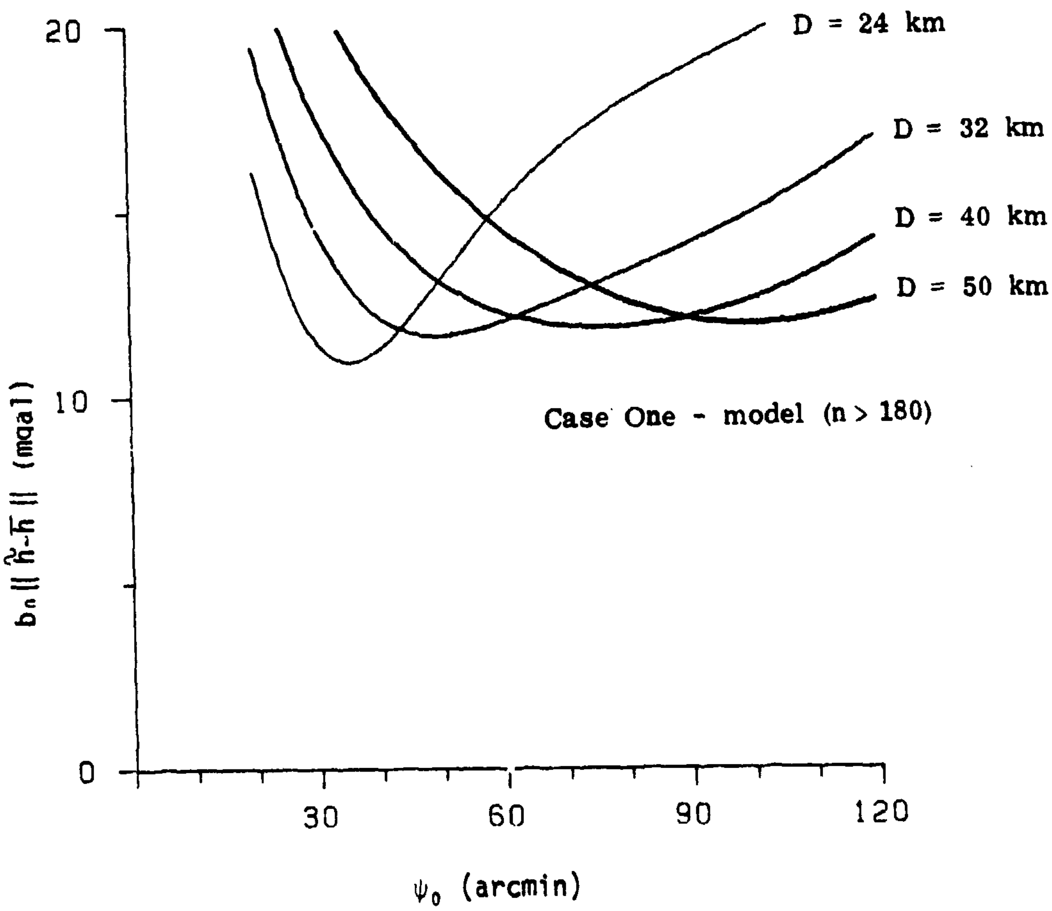

j. 4.5a rms values of $\delta\Delta g$ caused by $\tilde{h} \neq \bar{h}$.

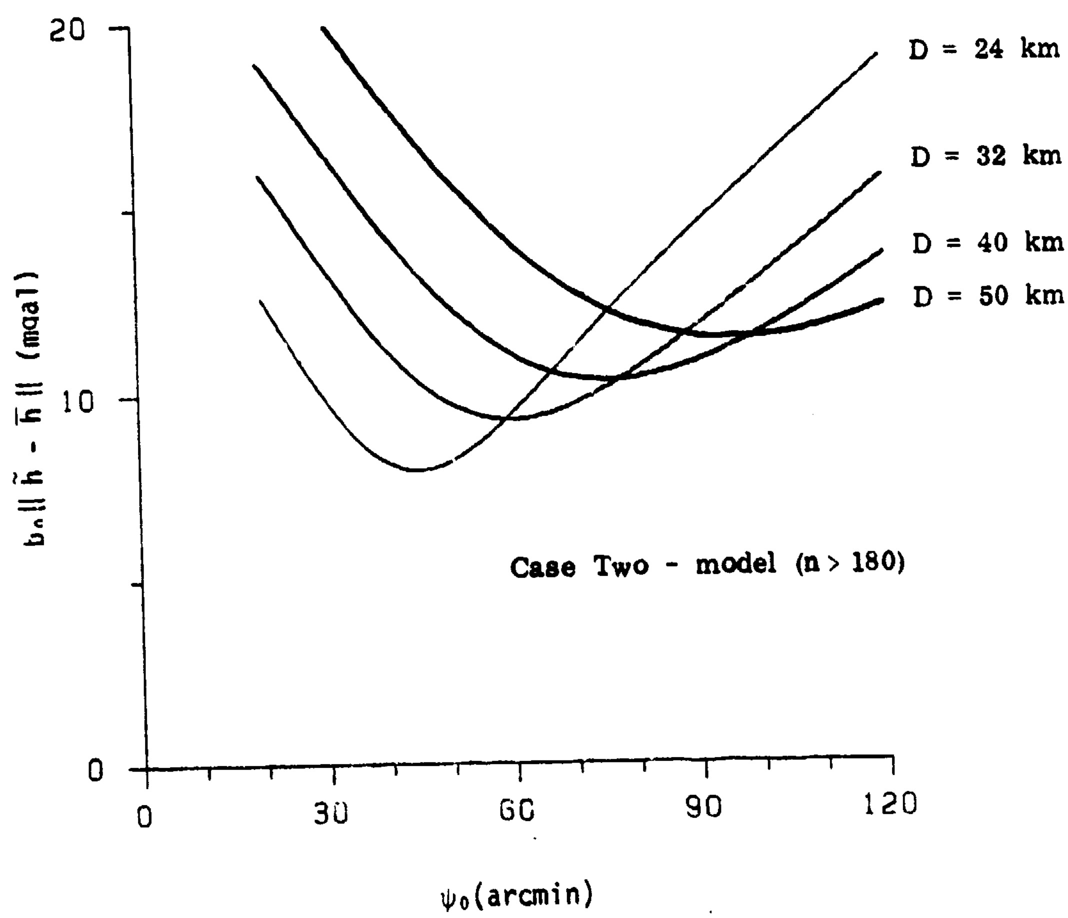

Fig. 4.5 b rms value of $\delta\Delta g$ caused by $\tilde{h} \neq \bar{h}$.

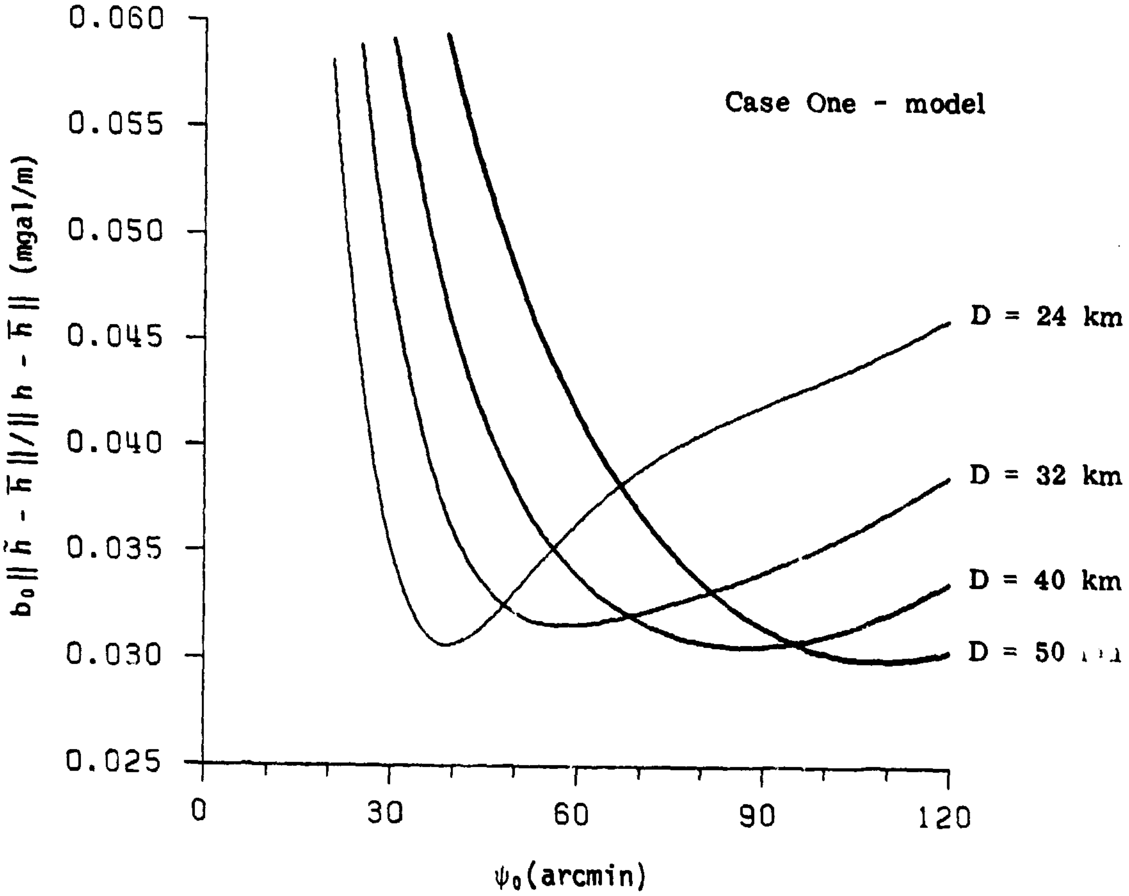

Fig. 4.6a Lower bound estimates of $\|\delta b\|$.

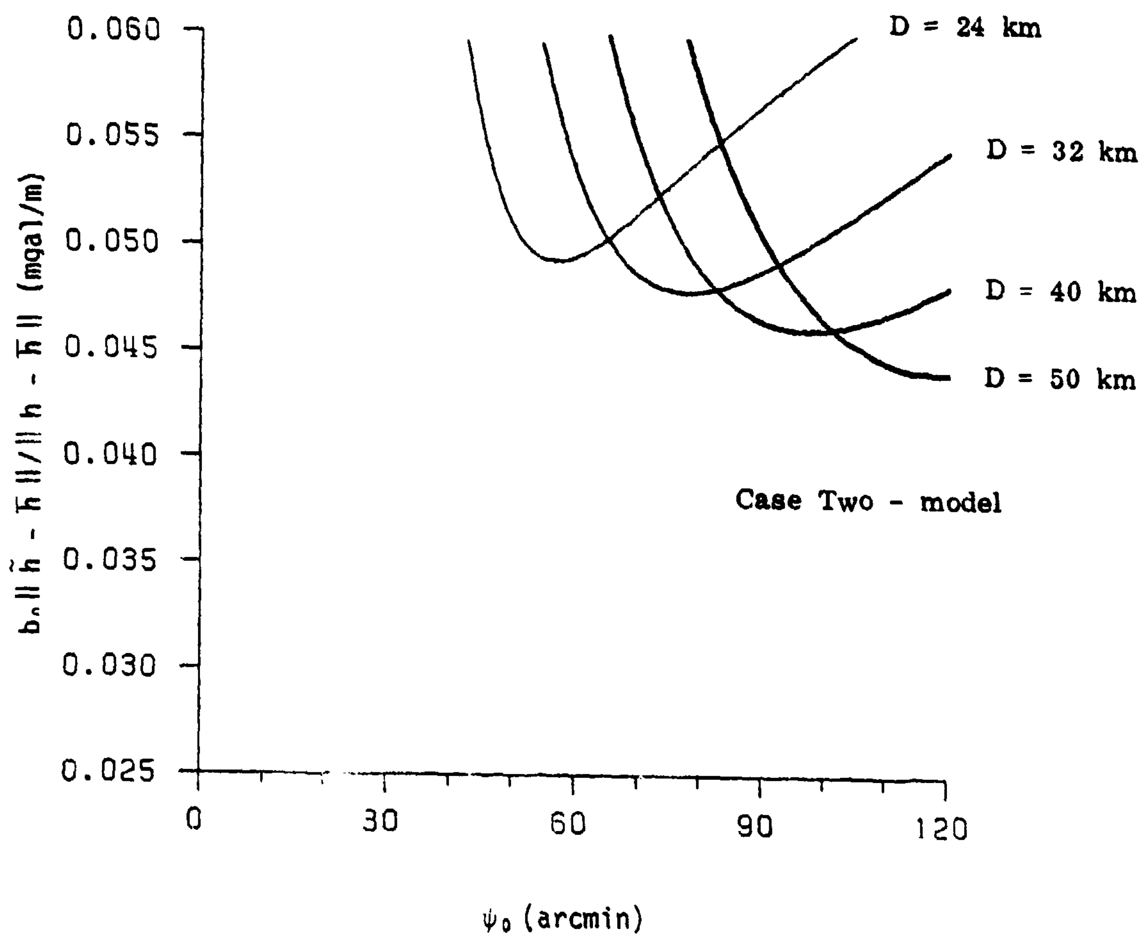

Fig. 4.6 b   Lower bound estimates of $||\delta b||$.

In the previous investigation of the error in b, caused by a replacement of $\tilde{h}$ by $\bar{h}$, only the global case has been considered. Therefore, the optimal estimates for ψ_0 should be interpreted with this reservation. Local optimal ψ_0 - values can be considerably smaller; therefore, the ψ_0 - estimates represent rather upper limits. Best local estimates depend on the individual situation; they could be obtained on the basis of a detailed digital terrain model.

Summarizing we can say that large deviations of b from the normal Bouguer gradient of 0.112 mgal/m can be expected if b is determined for a large block by least-squares adjustment and in addition, if the Bouguer anomaly is not constant within the block. Using a simplified concept of isostatic compensation, we could give a very simple mathematical explanation for this phenomena. If the least-squares adjustment concept is used for the estimation of b, the selection of an appropriate block size should be done very carefully. In general it is much better to choose a too small block size than a too large one; this is particularly true for mountainous areas. The least-squares collocation determination of b is quite insensitive with respect to the choice of the block size because it takes into account the variation of the Bouguer - anomaly within the block. Therefore, it is a very good advise to estimate b using the method of least-squares collocation with parameters, particularly in areas with sparse data coverage. In addition, collocation allows at the same time the estimation of the Bouguer anomaly field and even the prediction of surface free-air point and mean anomalies together with their accuracies. The author is not aware of any other nearly as powerful existing method.

5. THE TERRAIN EFFECT ON POINT ANOMALIES

The natural goal of estimation problems is to keep the error of estimation as small as possible. Least-squares interpolation, in particular, is sensitive with respect to the statistical properties of the field to be estimated, expressed in terms of a (usually) isotropic and homogeneous covariance function. The interpolation error depends strongly on a) the variance C_0 and b) on the ratio r = correlation length/data spacing (Sünkel, 1981). A small interpolation error is achieved by a small C_0 and a large r. Therefore, any data reduction process, which decreases the variance and increases the correlation length, has to be favorably considered. It is common sense that the irregularities of the topography account significantly in the power of first and higher order derivatives of the gravitational field. In particular, the free-air anomaly's high-frequent variation comes primarily from the influence of the topography. In other words, the topography makes C_0 increase and the correlation length decrease. This is why predictions in mountainous areas, based on unreduced free-air gravity field quantities, give poor accuracies. If we want to achieve high prediction accuracy, we have only two alternatives: do manpower-consuming expensive field work and collect more data just to make r increase, or reduce the data for the influence of the topography. Needless to say, plain mortal geodesists prefer the latter.

In linear and planar approximation the topographic correction of gravity at a surface point P is given by (Moritz, 1969, p. 10)

$$C_P = \tfrac{1}{2}\, G\rho R^2 \iint_\sigma \frac{(h - h_P)^2}{\ell_0^3}\, d\sigma \tag{5.1}$$

with $\ell_0 = 2R \sin \psi/2$. Since the integral kernel ℓ_0^{-3} drops rapidly to zero, only a very small region, centered at the computation point P, has to be considered for the evaluation of (5.1); therefore, it is legitimate to formally replace the sphere by its tangential plane at P.

In the following we shall investigate how detailed topographic information has to be made available in order to meet certain accuracy requirements. Let us first investigate the critical zone in the neighborhood of the computation point P. Following Heiskanen & Moritz (1967, p.121ff.), we represent the topography around P in terms of a Taylor series,

$$h(s,\alpha) = h_P + s(h_x \cos\alpha + h_y \sin\alpha) + \ldots; \tag{5.2}$$

here s and α denote the planar distance and the azimuth, x and y are cartesian coordinates. Then (5.1) is represented by

$$\delta C_P = \tfrac{1}{2}\, G\rho \int_{\alpha=0}^{2\pi} \int_{s=0}^{s_0} \frac{[h(s,\alpha)-h_P]^2}{s^3}\, s\, ds\, d\alpha \ ,$$

and with (5.2) we obtain, neglecting higher order terms,

$$\delta C_P = \tfrac{1}{2}\, G\rho \int_{\alpha=0}^{2\pi} \int_{s=0}^{s_0} (h_x^2 \cos^2\alpha + h_y^2 \sin^2\alpha + 2h_x h_y \sin\alpha \cos\alpha)\, ds\, d\alpha.$$

Due to the orthogonality relations of trigonometric functions, this expression reduces to the simple form

$$\delta C_P = \pi G \rho s_0 \tfrac{1}{2}(h_x^2 + h_y^2). \tag{5.3}$$

Consider e.g. a small zone with a radius $s_\bullet$ = 300 m and a moderate slope of 20° only, the terrain correction will assume a value of about 1 mgal. Consequently, the resolution of the used terrain model has to be very high in the neighborhood of the calculation point, unless P is located on a "flat spot" of the terrain.

In order to study the response of C to the terrain, we need terrain models. However, the choice of a proper terrain model is a very delicate problem. To some degree it can be anticipated that C will be relatively insensitive with respect to high-frequent, and sensitive with respect to medium-frequent topographic variations. As a matter of fact, C should depend somehow on the power of those variations. For the sake of simplicity we choose a very simple but instructive topographic model: an isotropic model represented by

$$h(s) = h_0 \cos \omega s, \tag{5.4}$$

centered at the computation point P; (note that $h_P = h_0$.) The model looks quite unnatural, but it isn't: imagine a gravity station either on a top of a mountain surrounded by (circular) mountain chains of comparable height which are separated by valleys, or - numerically equivalent- a gravity station in a valley surrounded by mountain chains and other valleys. The only unlikely structure in our model is the circular symmetry, constant amplitude and frequency. However, in order to study the influence of topography on gravity, sacrifices have to be made resulting in simple structures.

With (5.4) the topographic correction (5.1) is given by

$$C = \pi G \rho \, h_0^2 \int_{s=0}^{\infty} \frac{(\cos \omega s \ -1)^2}{s^2} ds. \tag{5.5}$$

(The integration over the azimuth has already been performed.) According to Ryshik and Gradstein (1963, p. 114, No. 2.523; p. 115, No. 2.526) the integral in (5.5) assumes the form

$$\int_{s=0}^{\infty} \frac{(\cos \omega s \ -1)^2}{s^2} ds = 2\omega^2 \left(\int_{s=0}^{\infty} \frac{\sin \omega s}{\omega s} ds - \int_{s=0}^{\infty} \frac{\sin 2 \omega s}{2 \omega s} ds \right)$$

$$+ \left[\frac{1}{s} \left(2 \cos \omega s - \tfrac{1}{2} \cos 2 \omega s - \tfrac{3}{2} \right) \right]_{s=0}^{\infty} .$$

The second expression [•] can easily be shown to vanish by a Taylor series evaluation at s=0. Considering

$$\int_0^{\infty} \frac{\sin px}{px} = \frac{\pi}{2p}$$

(Ryshik and Gradstein, 1963, p. 169, No. 3.522), the first expression (•) assumes the simple form $\pi/4\omega$; with $\omega = 2\pi/\lambda$ (λ ... wave-length), the topographic correction (5.5) is given by

$$C = \pi^3 G \rho \frac{h_0^2}{\lambda} \ . \tag{5.5'}$$

This remarkably simple result for the equally simple model deserves a discussion: Let us first reflect about its validity. Formula (5.1) represents the linear term of a series expansion of the topographic correction in planar approximation with respect to $[(h-h_P)/\ell_0]^2$, which essentially represents the square of the tangent of the elevation angle β of a variable terrain point with respect to P, $\tan^2\beta$. The series obviously converges if $|\beta| < 45^0$; therefore, equations (5.1) as well as (5.5)' are valid approximations for moderate terrain only with $\tan^2\beta$ significantly smaller than 1. In terms of the wavelength λ of our model, this translates into $\lambda > 4h_0$; in order to be absolutely save, we should rather write

$$C = \pi^3 G\rho \frac{h_0^2}{\lambda} \quad , \quad \lambda \gg 4h_0 \quad . \tag{5.5)''$$

C vanishes if $\lambda \to \infty$ as it should be. The most important result (at least for the model considered here) can be summarized as follows:

The topographic correction is proportional to the square of the amplitude h_0 (and consequently linearly dependent on the variance of the topography), and is inverse proportional to the wavelength λ of the topography, provided $\lambda \gg 4h_0$.

The following Table 5.1 shows C for our model, dependent on various choices of h_0 and λ.

h_0(m) \ λ(m)	100	1000	5000	10 000
10	0.55	0.05	0.01	<0.01
100		5.5	1.1	0.55
500			27.6	13.8
1000				55.2

Table 5.1 Topographic correction (mgal) dependent on amplitude h_0 and wavelength λ.

The figures obtained with our simple model agree remarkably well with real world observations; cf. Heiskanen and Vening Meinesz (1958, p. 154). (Note, for example, that the figure in the last line and last column corresponds to the situation of a mountain top 2000 m above the surrounding valley and having a circular basis of 20 km in diameter.) It is quite instructive to compare these values with figures derived from a cone model with height = 2 h_0 and base-radius = $\lambda/2$; the topographic correction can easily be shown to equal $C = 8\pi G\rho h_0^2/\lambda$; therefore, our two models differ only by $8/\pi^2 \doteq 0.8$ and consequently, the cone-model values corresponding to the figures in Table 5.1 are only 20% smaller; a very astonishing result, which both convinces the above rule of thumb and indicates the moderate influence of remote zones.

Let us still investigate another isotropic model represented by

$$h(s) = h_0 \sin \omega s, \tag{5.6}$$

centered at the computation point P; (note that $h_P = 0$.) With (5.1) the topographic correction is given by

$$C = \pi G\rho h_0^2 \int_{s=0}^{\infty} \frac{\sin^2 \omega s}{s^2}\, ds \quad ;$$

with (Ryshik and Gradstein, 1963, p. 166, No. 3.512) and $\omega = 2\pi/\lambda$ as before, we obtain

$$C = \pi^3 G\rho \frac{h_0^2}{\lambda} \quad , \lambda \gg 4\, h_0 \tag{5.7)'$$

which is identical to $(5.5)^{\sim}$.

As a last model we will consider a non-isotropic so-called "two-dimensional" model which has a constant profile in one direction,

$$h(x) = h_0 \sin \omega x; \tag{5.8}$$

the computation point is supposed to be located at x = 0. With (5.1) the topographic correction is given by

$$C = \tfrac{1}{2}\, G\rho h_0^2 \int_{x=-\infty}^{\infty} \int_{y=-\infty}^{\infty} \frac{\sin^2 \omega x \, dxdy}{\sqrt{x^2 + y^2}^{\,3}} \tag{5.9}$$

Due to the symmetry of the integrand with respect to x = 0 and y = o, C can also be expressed by

$$C = 2G\rho h_0^2 \int_{x=0}^{\infty} \int_{y=0}^{\infty} \frac{\sin^2 \omega x \, dxdy}{\sqrt{x^2 + y^2}^{\,3}} \tag{5.9)'$$

The integration with respect to y is very simple and yields

$$\int_{y=0}^{\infty} \frac{dy}{\sqrt{x^2 + y^2}^{\,3}} = \frac{1}{x^2 \sqrt{1 + \frac{x^2}{y^2}}} \Bigg|_{y=0}^{\infty} = \frac{1}{x^2} \quad ,$$

and therefore C reduces to

$$C = 2\, G \rho h_0^2 \int_{x=0}^{\infty} \frac{\sin^2 \omega x}{x^2}\, dx \quad ,$$

which differs from (5.7) only by a factor $2/\pi$ and we obtain with $\omega = 2\pi/\lambda$ as above

$$C = 2\pi^2 G\rho \frac{h_0^2}{\lambda} \quad , \lambda \gg 4\, h_0. \tag{5.9}$$

Also for this quite different model (note that the computation point is located at the slope of a mountain chain) we observe the same dependence on h_0^2 and λ. Therefore, we conclude that our rule of thumb

$$C = O(h_0^2/\lambda) \tag{5.10}$$

seems to be of general validity.

What is the logical consequence for the design of a digital terrain model for the purpose of reducing gravity measurements? Observing (5.10), the obvious answer is as follows: the terrain sampling rate must be selected terrain-specifically; rough terrain requires higher rates, smooth terrain lower sampling rates; it is not a good advice to keep the sampling rate globally constant. If we are talking about a rough terrain we mean not only small wavelengths but also high power; high-frequent terrain oscillations with a small amplitude need not be resolved, they should be smoothed out by an appropriate smoothing process; a mean value representation over rectangular blocks or even a mean value reproducing smooth representation should be favorably considered. The block size, in turn, depends strongly on the power of the high-frequent portion of the terrain spectrum, and in addition on the desired accuracy of the terrain correction.

The terrain correction (5.1) can also be represented in terms of polar coordinates (ψ,α)

$$C_P = \frac{G\rho}{2R} \int_{\psi=0}^{\pi} \int_{\alpha=0}^{2\pi} \frac{\left[h(\psi,\alpha)-h_P\right]^2}{\ell_0^3(\psi)} \sin\psi d\psi d\alpha. \tag{5.11}$$

Performing the integration with respect to the azimuth α first (for a fixed spherical distance ψ), and denoting the mean square height difference (with respect to h) by $h^{*2}(\psi)$,

$$h^{*2}(\psi) = \frac{1}{2\pi} \int_{\alpha=0}^{2\pi} \left[h(\psi,\alpha)- h_P\right]^2 d\alpha, \tag{5.12}$$

the terrain correction may be written

$$C_P = \frac{\pi G\rho}{R} \int_{\psi=0}^{\pi} \frac{h^{*2}(\psi)}{\ell_0^3(\psi)} \sin\psi d\psi. \tag{5.11$'$}$$

Observing the rapid decrease of the function $\sin\psi/\ell_0^3(\psi)$, expression (5.11)$'$ can be considerably simplified for practical applications; with

$$\frac{\sin\psi}{\ell_0^3(\psi)} = \frac{2\sin\psi/2\cdot\cos\psi/2}{8\sin^3\psi/2} \doteq \frac{1}{\psi^2}$$

for small ψ, (5.11)$'$ is given by

$$C_P = \frac{\pi G\rho}{R} \int_{\psi=0}^{\psi_0} \frac{h^{*2}(\psi)}{\psi^2} d\psi. \tag{5.11$''$}$$

(ψ_0 = $1^{\circ}5$ is sufficient in any case (Hay-Ford zone O); cf. (Heiskanen and Vening Meinesz, 1958, p. 154).) In terms of the linear distance $s = R\psi$, above formula is written

$$C = \pi G \rho \int_{s=0}^{s_0} \frac{h^{*2}(s)}{s^2}\, ds, \qquad (5.11)''$$

Let us now recall the isotropic terrain model (5.4) discussed earlier. Comparing (5.5) with (5.11)" , we observe that our requirements can be considerably relaxed: the model has to be such that only its mean square value (extended over the azimuth α; s fixed) behaves like $h_0^2 \left(\cos \frac{2\pi}{\lambda} s-1\right)^2$, otherwise it is largely arbitrary. Consider the integrand of (5.5): with a constant denominator the maximum would be attained at $s = (2k+1)\lambda/2$, $k = 0, 1, \ldots$. Due to the rapidly increasing denominator s^2, the maximum of the composite integrand is shifted to smaller values of s; in addition, C gets its power mainly from the region of the inegrand's first maximum; local maxima of larger s contribute very little to the terrain effect. This is why the simple cone model discussed above differs only little from the model (5.4) as far as the terrain effect is concerned. Fig. 5.1 illustrates the behavior of the integrand corresponding to model (5.4) for various wavelengths (common h_0, normalized). It is quite remarkable that these graphs, despite of the underlying model's simplicity, agree favorably well with graphs derived from real world topography; cf. (Mathisen, 1976); this fact confirms once more the h_0^2/λ - law.

The practical consequences are as follows: the location of the first maximum is strongly influenced by the variation of the topography in the neighborhood of the computation point; therefore a very detailed

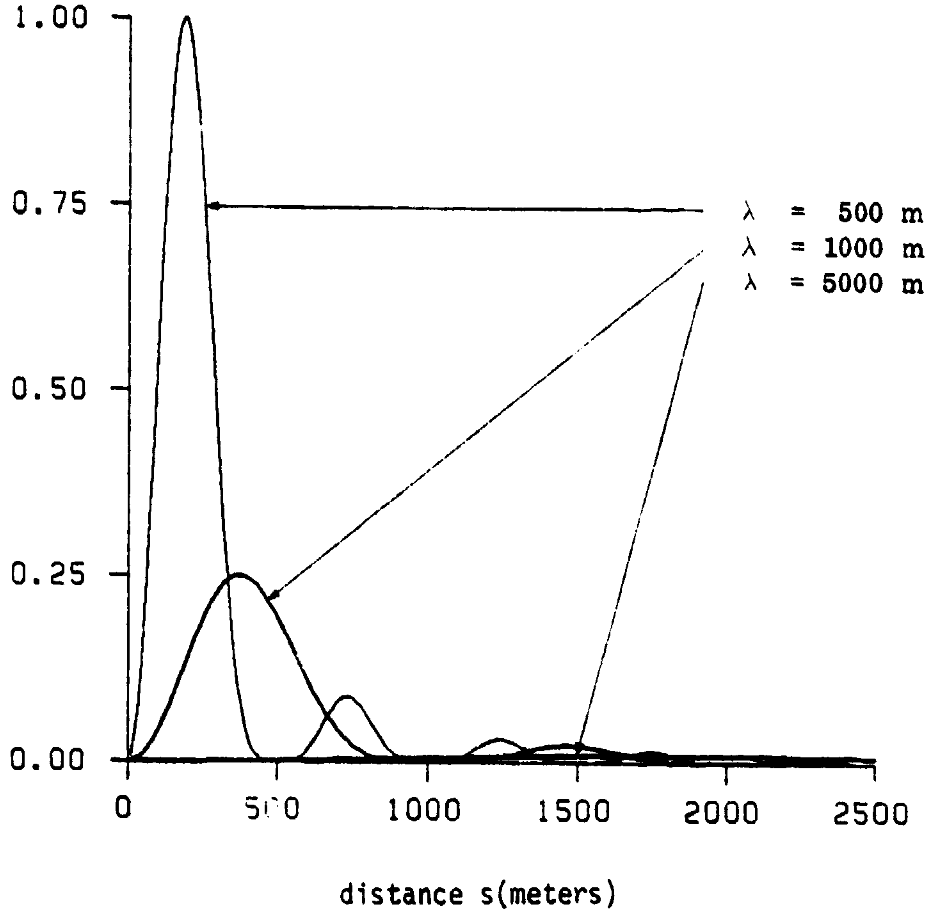

Fig. 5.1 Integrand $[h_0(\cos \frac{2\pi}{\lambda} s - 1)/s]^2$ for various wavelengths λ.

digital terrain model (DTM) is required in this region, unless the computation point is located at a flat spot of the topography. The degree of resolution of the DTM, therefore, depends on three essential factors:

a) on the variance of the terrain surrounding the computation point P,

b) on the wavelength of the terrain surrounding P,

c) on the location of the first maximum of the integrand in (5.11)" .

Table (5.1) and Fig. (5.1) provide us with a rough guideline for a proper choice of the required DTM's resolution; however, the decision must be made on individual circumstances.

6. THE EFFECT OF TOPOGRAPHY ON MEAN ANOMALIES

Mean free-air anomalies as defined by (2.2) can be split up into two components: the mean Faye anomaly plus a mean terrain correction. Chapters 2 and 3 deal with the estimation of point and mean Faye anomalies; chapter 5 considers essential aspects concerning the calculation of point terrain corrections. As a matter of fact, the effect of topography on mean anomalies equals the mean terrain effect; its estimation will be discussed in the sequel.

The most straightforward way of estimating the mean terrain effect is to calculate a dense grid of point terrain effects and take the average. The calculation of the point terrain effect requires the evaluation of an integral formula like (5.1), an expensive task even for high-speed computer. Note that equation (5.1) is of "differentiation type" which can be clearly seen by observing its behavior in the innermost zone surrounding the computation point P. The mean terrain effect is obtained by integrating the point terrain effects. Do we really have to suffer from the instabilities of differentiation first before we can enjoy the stability of integration? There must be a direct and inexpensive solution to the problem of mean terrain correction estimation which avoids the up's and down's of differentiation + integration. (A very similar problem is encountered in connection with the astrogeodetic determination of the geoid: plumb-line curvature correction and orthometric reduction; see Heiskanen & Moritz, 1967, pp. 200, 201.)

Let us consider the terrain correction as given by equation (5.11)'. The mean terrain correction $\overline{C} = M\{C\}$ is obviously obtained by averaging

the point terrain corrections within the area $\Delta\sigma$ of consideration,

$$\bar{C} = \frac{1}{\Delta\sigma} \iint\limits_{\Delta\sigma} C d\sigma \quad . \tag{6.1}$$

Let us try to formulate the procedure of calculating $\bar{C}$:

a) keep a circle with radius $= \psi$ fixed;

b) keep a point $P \varepsilon \Delta \sigma$ fixed and make it the center of the circle;

c) calculate the mean square height differences as defined by (5.12) for this particular circle;

d) change P and repeat (b) and (c) until $\Delta\sigma$ is covered;

e) calculate the average of all outcomes of (c);

f) change ψ and repeat (a) - (e) until $[0, \psi_0]$ is covered with an appropriate ψ_0 (e.g. $1^{\circ}5$);

g) perform (5.11) .

In terms of a formula it can be written as

$$\bar{C} = \frac{\pi G \rho}{R} \int\limits_{\psi=0}^{\psi_0} \left\{ \frac{1}{\Delta\sigma} \iint\limits_{\Delta\sigma} \frac{1}{2\pi} \int\limits_{\alpha=0}^{2\pi} \Delta h^2 d\alpha \right\} \frac{d\psi}{\psi^2} \tag{6.2}$$

The expression $\{\cdot\}$ represents (c) - (e) and equals the variance of height differences between two surface points, separated by a distance ψ, for the individual area $\Delta\sigma$ in consideration.(1) This variance is related to the elevation auto-covariance function $H(\psi)$ as follows:

$$\frac{1}{2\pi\Delta\sigma} \int\limits_{\alpha=0}^{2\pi} \iint\limits_{\Delta\sigma} \Delta h^2 d\sigma d\alpha = 2\left[H_0 - H(\psi)\right] \text{ , } H_0 = H(0) . \tag{6.3}$$

(1) ... provided $\Delta\sigma$ is sufficiently larger than ψ_0

Replacing the spherical by planar expression, we obtain the very simple expression

$$\bar{C} = 2\pi G\rho \int_{s=0}^{s_0} \frac{[H_0 - H(s)]}{s^2}\, ds \quad . \tag{6.4}$$

In the following we will evaluate this integral for various covariance functions, the generalized Hirvonen models and the Gaussian covariance function.

a) The classical Hirvonen model

$$H(s) = \frac{H_0}{1+\left(\frac{s}{\xi}\right)^2} \quad , \tag{6.5a}$$

where ξ denotes the correlation length, yields an integral (Ryshik and Gradstein, 1963, p. 60, No. 2.141)

$$\int_{s=0}^{\infty} \frac{H_0 - H(s)}{s^2}\, ds = \frac{H_0 \pi}{2\xi}$$

and we obtain for the mean terrain correction the value

$$\bar{C} = \pi^2 G\rho \frac{H_0}{\xi} \tag{6.6a}$$

b) The second Hirvonen model has been discussed in Moritz (1980),

$$H(s) = \frac{H_0}{\left[1+\left(\frac{s}{a}\right)^2\right]^{\frac{1}{2}}} \quad , \tag{6.5b}$$

where the parameter a is related to the correlation length ξ through $\xi = a\sqrt{3}$.

$$\int_{s=0}^{\infty} \frac{H_0 - H(s)}{s^2}\, ds = \frac{H_0}{a}$$

and we obtain for $\overline{C}$ the value

$$\overline{C} = 2\sqrt{3}\,\pi G\rho \frac{H_0}{\xi} \quad . \tag{6.6b}$$

c) The last Hirvonen covariance model (Moritz, 1980) is

$$H(s) = \frac{H_0}{\left[1 + \left(\frac{s}{a}\right)^2\right]^{3/2}} \quad , \tag{6.5c}$$

where the parameter a is related to the correlation length ξ through $\xi = a(2^{2/3} - 1)^{1/2}$. According to Ryshik and Gradstein (1963, p. 82, No. 2.268) the integral yields

$$\int_{s=0}^{\infty} \frac{H_0 - H(s)}{s^2}\, ds = \frac{2\, H_0}{a}$$

and we obtain for $\overline{C}$ the expression

$$\overline{C} = 4\sqrt{2^{2/3} - 1}\;\pi G\rho \frac{H_0}{\xi} \;. \tag{6.6c}$$

d) The Gaussian covariance model

$$H(s) = H_0 e^{-a^2 s^2} \tag{6.5d}$$

has a correlation length $\xi = \frac{1}{a}\sqrt{\ln 2}$ and yields an integral (Ryshik and Gradstein, 1963, p. 151, No. 3.273)

$$\int\limits_{s=0}^{\infty} \frac{H_0 - H(s)}{s^2}\, ds = \sqrt{\pi}\ \frac{H_0}{a}$$

and we obtain for the mean terrain correction the value

$$\overline{C} = 2\sqrt{\pi \ \ln 2}\ \ \pi G\rho \frac{H_0}{\xi} \quad . \tag{6.6d}$$

In ll four covariance models we observe the common factor $\pi G\rho \frac{H_0}{\xi}$. The model-specific multiplication factor is shown in Table 6.1.

Covariance model	C_0
Hirvonen (a)	$\pi \quad = 3.14$
Hirvonen (b)	$2\sqrt{3} \quad = 3.46$
Hirvonen (c)	$4\sqrt{2^{2/3}-1} \quad = 3.07$
Gauss	$2\sqrt{\pi\ \ln 2} \quad = 2.95$

Table 6.1 Model-specific multiplication factors,
$\overline{C} = C_0 \cdot \pi G\rho \frac{H_0}{\xi}$.

We notice that for all four models the mean terrain correction $\overline{C}$ varies in a very narrow range with variations of only 10%. Therefore, we conclude that the estimation of $\overline{C}$ is only little sensitive with respect to the model choice. We summarize:

The mean terrain correction depends linearly on the terrain variance and is inverse proportional to the correlation length of the terrain covariance function valid for the considered area. It depends weakly on the type of the covariance model.

This very interesting and astonishingly simple result deserves a discussion. The variance of the height differences as defined by (6.3) is valid for the area $\Delta\sigma$ in consideration; therefore, the terrain covariance function H(s) has to be derived from topographic data in the same limited area only. In flat areas the variance of the topography is small and the correlation length big, resuiting in a very small mean terrain effect as to be expected. In mountainous areas, in constrast, we observe a big variance and a small correlation length, resulting in a very significant mean terrain effect as also to be expected. How does it come that, according to equations (6.6a-d), the mean terrain effect is virtually independent on the size of the area $\Delta\sigma$? The answer is simple: the area size $\Delta\sigma$ lurks in the background and is implicitly introduced through the definition and determination of the covariance parameters H_0 and ξ. It is known from experience that the terrain variance and correlation length can considerably change with the size of the area $\Delta\sigma$. If $\Delta\sigma$ increases, the correlation length will in general increase too. H_0 can attain quite large values; in mountainous areas values of H_0 = 0.5 to 1 km^2 can be observed; the correlation length of the terrain covariance function is usually much smaller than the one of the free-air anomaly covariance function; particularly in mountainous areas it can be as small as a very few kilometers. Fig. 6.1 shows lines of equal mean terrain effect

depending on the r.m.s. elevation and the correlation length ξ for the Hirvonen (a) - model; Fig. 6.2 is a 3-D representation of the behavior of (6.6a).

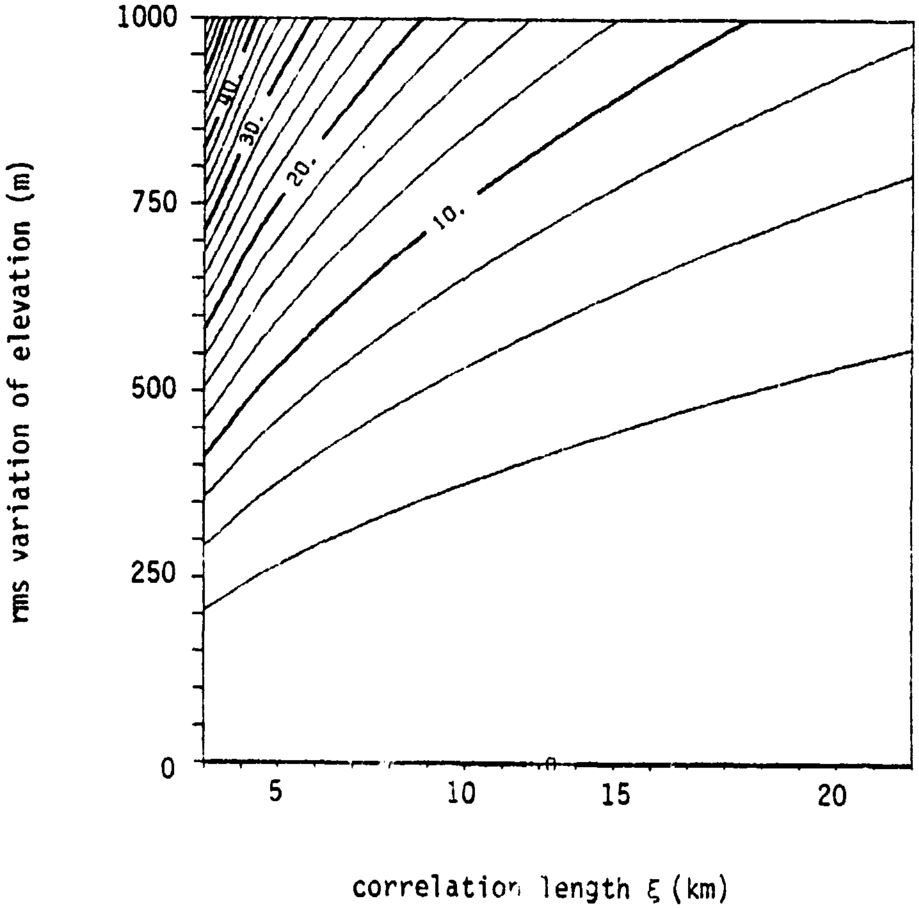

Fig. 6.1 Lines of equal mean terrain effect depending on the r.m.s. variation of elevation and the correlation length ξ for the Hirvonen (a)-model.
unit: mgal

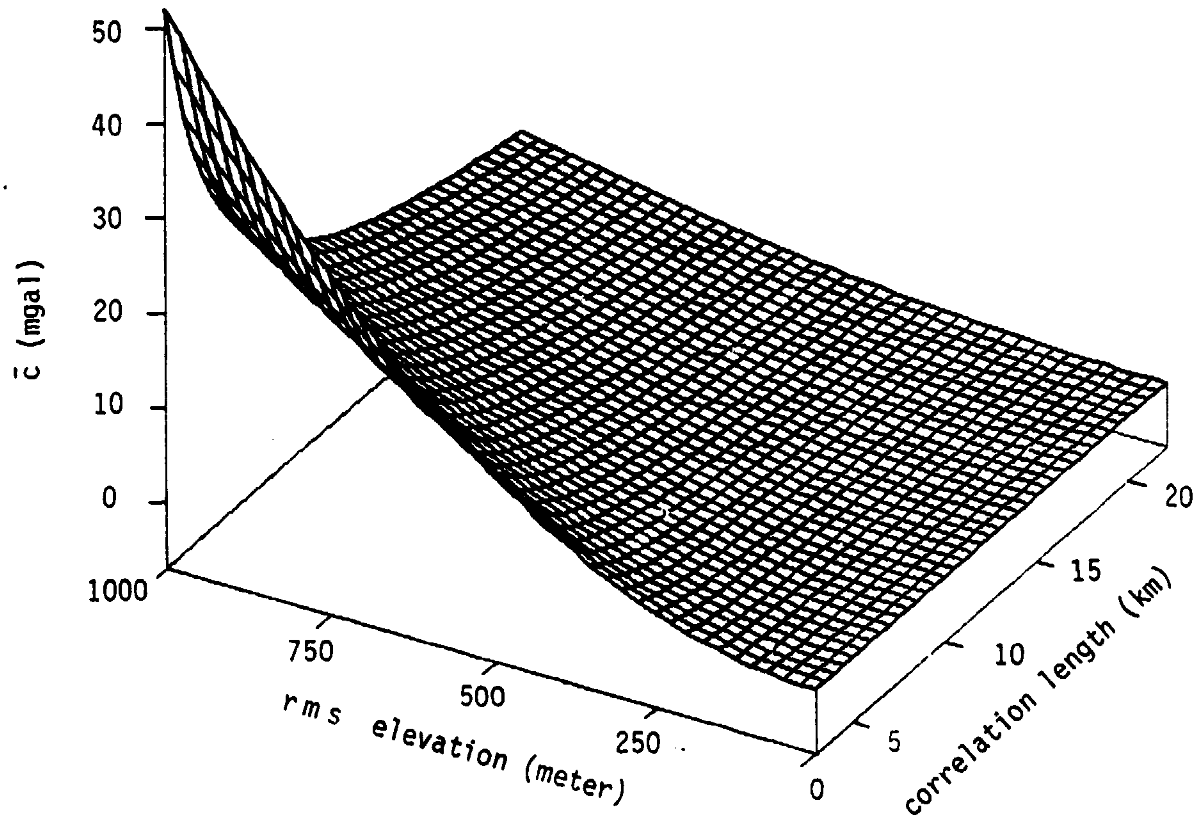

Fig. 6.2 Mean terrain effect (mgal) for the Hirvonen (a) covariance model

7. CONCLUSIONS AND RECOMMENDATIONS

Different methods have become available for the prediction of point and mean free-air anomalies based on observed point anomalies. By far the most attractive, but also most expensive, tool is least-squares prediction. The most general version of least-squares gravity prediction involves the processing of gravity and elevation data simultaneously. In this report a least-squares approach is proposed, which takes the generally observed strong linear correlation between (terrain reduced) free-air anomalies and elevation into account in terms of two model parameters; the method is therefore based on least-squares collocation with parameters. The signal is basically a residual Bouguer anomaly and such is the corresponding covariance function. Bouguer anomalies are smooth, therefore, the covariance function has a rather long correlation length; consequently, the interpolation (prediction) accuracy is high. It has been shown that a regional variation of the Bouguer anomaly causes the Bouguer factor to decrease if a regional least-squares adjustment is used; in addition its estimation accuracy becomes very poor. The collocation solution, in contrast, models the Bouguer anomaly field statistically and provides highly reliable estimates of the Bouguer factor which turned out to be generally quite close to its normal value. Particularly important for free-air anomaly predictions in mountainous areas, is the data reduction for the influence of the topography. Various simple, but instructive, topographical models have been studied. It turned out that the mean terrain effect is linearly dependent on the variance and indirectly proportional to the correlation length of the residual topography within the area of consideration. Therefore, the accuracy of its determination depends on how good

the estimates of the terrain variance and the terrain correlation length are.

Summarizing we propose the following method for mean free-air gravity anomaly estimation:

a) Reduce gravity data for the terrain effect;

b) determine an empirical covariance function and fit a model;

c) determine the correlation model parameters (mean Bouguer anomaly and the Bouguer factor) by least-squares collocation;

d) predict point and/or mean anomalies by least-squares collocation with parameters;

e) add the point and/or mean terrain effect to the obtained estimate in order to get free-air anomalies.

Predictions with real world data have shown that free-air 5' x 5' anomalies, even in very rough mountainous areas, can be predicted with an accuracy of $< \pm 5$ mgal. using the method proposed above, provided the data density is better than 1/10 km^2 and the effect of topography has been carefully taken into account.

Further investigation, particularly as far as the resolution of the digital terrain model is concerned, are both useful and necessary.

REFERENCES

Faddeeva, V. N. (1959): Computational Methods of Linear Algebra. Dover Publications, New York.

Heiskanen, W. A. and F. A. Vening Meinesz (1958): The Earth and its Gravity Field. McGraw-Hill, New York.

Heiskanen, W. A. and H. Moritz (1967): Physical Geodesy. W. H. Freeman, San Francisco.

Jekeli, C. (1978): An investigation of two models for the degree variances of global covariance functions. Report No. 275, Department of Geodetic Science, The Ohio State University, Columbus, Ohio.

Mathisen, O. (1976): A method for Bouguer reduction with rapid calculation of terrain corrections. Geodetic Publications, No. 18, Geographical Survey of Norway.

Meissl, P. (1971): Preparations for the numerical evaluation of second order Molodensky - type formulas. Report No. 163, Department of Geodetic Science, The Ohio State University, Columbus, Ohio.

Moritz, H. (1963): Interpolation and prediction of point gravity anomalies of $1^{\circ} \times 1^{\circ}$ blocks. Report No. 95, Department of Geodetic Science, The Ohio State University, Columbus, Ohio.

Moritz, H. (1969): Uber die Verwendung der Geländekorrektion fur Lösung des Problems von Molodenski. DGK - Reihe A., Heft Nr. 63, München.

Moritz, H. (1977): On the computation of a global covariance model. Report No. 255, Department of Geodetic Science, The Ohio State University, Columbus, Ohio.

Moritz, H. (1980): Advanced Physical Geodesy. H. Wichmann Verlag, Karlsruhe.

Müller, C. (1966): Spherical harmonics. Lecture Notes in Mathematics, No. 17, Springer-Verlag, Berlin.

Rapp, R. H. (1979): Potential coefficient and anomaly degree variance modelling revisited. Report No. 293, Department of Geodetic Science, The Ohio State University, Columbus, Ohio.

Rapp, R. H. (1981): High degree spectrums of the earth's potential, topography and its isostatic compensation. Unpublished manuscript. Department of Geodetic Science, The Onio State University, Columbus, Ohio.

Ryshik, I. M. and I. S. Gradstein (1963): Tables of Series, Products, and Integrals. VEB Deutscher Verlag der Wissen schaften, Berlin.

Sjöberg, L. (1980): A recurrence relation for the β_n - function. Bull. Geod. 54, pp. 69 - 72.

Sünkel, H. (1981): Cardinal Interpolation. Report No. 312, Department of Geodetic Science, The Ohio State University, Columbus, Ohio.

Sünkel, H. und R. Malits (1981): Höhen korrelation, Kovarianzfunktion und Prädiktion von Schwere anomalien in lokal begrenzten Gebieten Österreichs. ÖZFV, 69. Jahrgang, Heft 1, S. 17 - 31.

Uotila, U.A. (1967a): Analysis of correlation between free-air anomalies and elevations. Report No. 94, Department of Geodetic Science, The Ohio State University, Columbus, Ohio.

Uotila, U.A. (1967b): Computation of mean anomalies of $1^\circ \times 1^\circ$ blocks. Report No. 95, Department of Geodetic Science, The Ohio State University, Columbus, Ohio.

ACKNOWLEDGEMENTS

The author wishes to thank his colleagues at the Institute of Theoretical Geodesy, Technical University graz, and at the Department of Geodetic Science and Surveying, The Ohio State University, for fruitful discussions and valuable comments.

Computer time has been made available by the Construction and Research Computer Center of The Ohio State University and by the EDV-Zentrum Graz.